NON-NASA
IN-05
293256
60P

DOT/FAA/CT-88/15

FAA Technical Center
Atlantic City International Airport
N.J. 08405

The Effect of Aircraft Size on Cabin Floor Dynamic Pulses

Gil Wittlin

Lockheed Aeronautical Systems Company
Burbank, California

Larry Neri

FAA Technical Center

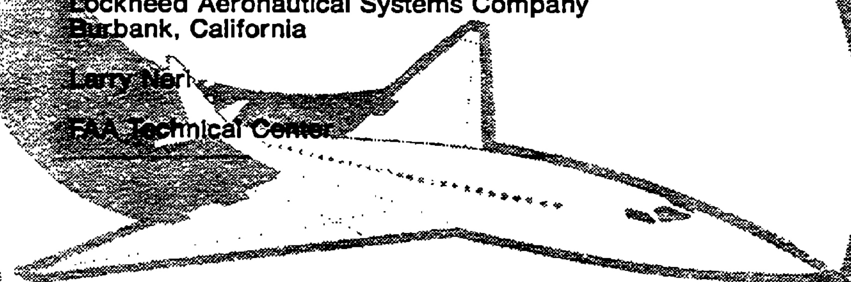

March 1990

Final Report

U.S. Department of Transportation
Federal Aviation Administration

Technical Report Documentation Page

1. Report No.	2. Government Accession No.	3. Recipient's Catalog No.
DOT/FAA/CT-88/15		

4. Title and Subtitle	5. Report Date / 6. Performing Organization Code / 8. Performing Organization Report No.
THE EFFECT OF AIRCRAFT SIZE ON FLOOR DYNAMIC PULSES	5. Report Date: March 1990
	6. Performing Organization Code: ACD-210
7. Author(s): G. Wittlin and L. Neri	8. Performing Organization Report No.: LR 31426
9. Performing Organization Name and Address: Lockheed Aeronautical Systems Company, Burbank, CA 91520/ Federal Aviation Administration Technical Center Atlantic City International Airport, NJ 08405	10. Work Unit No. (TRAIS)
	11. Contract or Grant No.: DTFA03-84-C-00004
12. Sponsoring Agency Name and Address: U. S. Department of Transportation Federal Aviation Administration Technical Center Atlantic City International Airport, NJ 08405	13. Type of Report and Period Covered: Final Oct 1987 - Dec 1989
	14. Sponsoring Agency Code: ACD-210

15. Supplementary Notes

16. Abstract

~~This report reviews and updates~~ size scaling trends. ~~It presents~~ an investigation into the effect that airplane size has on dynamic floor pulses generated within the cabin during a crash impact event. ~~and includes:~~

(1) A review of narrow-body and wide-body section test results and supporting analytical model results;

(2) The utilization of the Controlled Impact Demonstration (CID) validated KRASH model to perform additional parametric studies;

(3) Defined relationships between parameters which influence aircraft structure dynamic response;

(4) Developed airplane preliminary size effect trend curves for floor dynamic pulses in terms of triangular pulse magnitudes, velocity changes and pulse duration.

A simple approximate expression relating aircraft fuselage crush energy dissipation and kinetic energy ~~was~~ utilized to generate a set of triangular pulse velocity - crush distance - peak acceleration curves. Estimated effective crush distances for various classes of airplane sizes or categories and available acceleration, velocity and crush data ~~were~~ plotted. Plots for vertical-direction and longitudinal-direction are presented.

17. Key Words	18. Distribution Statement
Floor Pulses, Dynamic Response, Vertical Pulse, Longitudinal Pulse, Analysis, KRASH, Crash Design Criteria, Fuselage Crush, Full-scale Crash Test Data, Section Test Data	Document is available to the public through the National Technical Information Service, Springfield, Virginia 22161

19. Security Classif. (of this report)	20. Security Classif. (of this page)	21. No. of Pages	22. Price
UNCLASSIFIED	UNCLASSIFIED	52	

Form DOT F 1700.7 (8-72) Reproduction of completed page authorized

TABLE OF CONTENTS

LIST OF FIGURES

LIST OF TABLES

EXECUTIVE SUMMARY

The FAA has recently published final rules addressing occupant safety (references 1, 2, 3, and 4). The revised FAA regulations introduce dynamic test requirements for seats in the form of acceleration versus time triangular pulses. A previous FAA sponsored study (DOT/FAA/CT-83/23, reference 13) addressed the effect airplane mass and size would have on floor pulses. Since the release of that report, additional data, in the form of section test and full-scale airplane test results, as well as an analytical study (DOT/FAA/CT-87/13, reference 17) addressing airplane crash design envelopes, have been obtained.

This report reviews and updates size scaling trends. An investigation was undertaken to determine the effect that airplane size has on dynamic floor pulses generated within the cabin during a crash impact event and includes:

- A review of narrow-body and wide-body section test results and supporting analytical model results.
- The utilization of the Controlled Impact Demonstration (CID) validated KRASH model to perform additional parametric studies.
- The definition of relationships between parameters which influence aircraft structure dynamic response.
- The development airplane preliminary size effect trend curves for floor dynamic pulses in terms of triangular pulse magnitudes, velocity changes and pulse duration.

A simple approximate expression relating aircraft fuselage crush energy dissipation and kinetic energy was utilized to generate a set of triangular pulse velocity - crush distance - peak acceleration curves. Estimated effective crush distances for various classes of airplane sizes or categories and available acceleration, velocity and crush data were plotted. Plots for vertical-direction and longitudinal-direction are presented. A preliminary size trend curve range is established for each of the two directional pulses. The vertical pulse trend curves are based on enveloping all the applicable measured and analytically developed data. The longitudinal trend curves assume that the survivable envelope ranges from the fringes of known survivable conditions to nonsurvivable crash test results.

The size effect study emphasizes that the results are more configuration sensitive and not directly related to mass. Large airplanes with limited effective crush regions could behave more like some smaller airplanes with regard to floor pulse.

1. INTRODUCTION

1.1 BACKGROUND

Several Federal Aviation Administration (FAA) regulatory actions addressing improved occupant safety issues, including the dynamic testing of seats, have been published between December 1986 and May 1988. A summary of seat dynamic test criteria for the different civil aircraft categories identified in these actions is shown in table 1. Final rules have been issued for FAR Part 23, excluding the commuter category (reference 1) and for Parts 27 and 29 (reference 2) rotorcraft. In addition an NPRM has been issued (reference 3) to require retrofit of all seats on transport category airplanes used in air carrier operations and transport category airplanes used in scheduled interstate service to comply with the recent FAR Part 25 amendment affecting dynamic test criteria (reference 4).

Federal Aviation Regulation (FAR) Part 23, (reference 5) identifies airworthiness standards for airplanes that have a Maximum Design (Certification) Takeoff Weight (MD(C)TW) of 12,500 pounds or less and a seating configuration of, excluding pilot seats, nine or less (normal, utility and acrobatic categories) and the newly defined commuter category (propeller driven multiengine airplanes having a seating configuration, excluding pilot seats, of 19 or less and a MD(C)TW of 19,000 pounds or less). FAR Part 25 (reference 6) prescribes airworthiness standards for transport category airplanes which range up to more than 700,000 pounds. FAR Part 27 (reference 7) and Part 29 (reference 8) prescribe airworthiness standards for normal category (MD(C)TW or 6000 pounds or less) and transport category rotorcraft, respectively.

Table 2 compares the recently amended FAR Part 25 transport category airplane criteria with that for amended Part 23 small airplanes. The data in table 2 suggest that small airplanes exposed to a survivable crash

TABLE 1. SEAT DYNAMIC TEST REGULATORY CRITERIA FOR CIVIL AIRCRAFT

DYNAMIC TEST REQUIREMENTS	PART 23 AMENDMENT	PART 25 AMENDMENT	PART 27 AMENDMENT	PART 29 AMENDMENT
TEST 1				
TEST VELOCITY (FT/SEC)	31	35	30	30
SEAT PITCH ANGLE (°)	60	60	60	60
SEAT YAW ANGLE (°)	0	0	0	0
PEAK DECEL. (G's)	19/15	14	30	30
TIME TO PEAK (SECONDS)	0.05/0.06	0.08	0.031	0.031
FLOOR DEFORMATION	NONE	NONE	10° PITCH/ 10° ROLL	10° PITCH/ 10° ROLL
TEST 2				
TEST VELOCITY (FT/SEC)	42	44	42	42
SEAT PITCH ANGLE (°)	0	0	0	0
SEAT YAW ANGLE (°)	10	10	10	10
PEAK DECEL. (G's)	26/21	16	18.4	18.4
TIME TO PEAK (SECONDS)	0.05/0.06	0.09	0.071	0.071
FLOOR DEFORMATION	10° PITCH/ 10° ROLL	10° PITCH/ 10° ROLL	10° PITCH/ 10° ROLL	10° PITCH/ 10° ROLL
COMPLIANCE CRITERIA				
MAX HIC	1000	1000	1000	1000
LUMBAR LOAD (LBS)	1500	1500	1500	1500
STRAP LOADS (LBS)	1750/2000	1750/2000	1750/2000	1750/2000
FEMUR LOADS (LBS)	N/A	2250	N/A	N/A
SAFETY BELT ON PELVIS	YES	YES	YES	YES
SHOULDER HARNESS ON SHOULDER	YES	YES	YES	YES
SEAT RESTRAINS DUMMY	YES	YES	YES	YES
SEAT STRUCTURE INTACT	YES	YES	YES	YES
SUPPORT STRUCTURE INTACT	YES	YES	YES	YES
FEDERAL REGISTER DATE	8/15/88	5/17/88	11/13/89	11/13/89

environment experience cabin floor pulses of higher vertical peak g's and shorter durations than the heavier, larger, and deeper (underfloor depth) transport category airplanes. The latter category aircraft can be more than 60 times heavier and with a fuselage which is significantly longer, wider, and deeper. A previous study, in which mass and size effects were investigated (reference 9), suggested such a trend (figure 1). The premises, conditions, and results of that study are shown in Appendix A. However, since that study (reference 9) was performed, there have been several fuselage section tests (references 10 through 14), the Controlled Impact Demonstration (CID) Test (reference 15), and several supporting analyses and other test results published (references 16-22). In light of the availability of additional data and analyses, a review and update of mass and size scaling trends is appropriate.

TABLE 2. AMENDED FAR 23 (EXCLUDING COMMUTER CATEGORY AIRPLANES) AND AMENDED FAR 25 SEAT DYNAMIC TEST REQUIREMENTS

	FAR 23			FAR 25	
	COMBINED		VERTICAL COMPONENT	COMBINED	VERTICAL
VERTICAL (60° PITCH)	FRONT	OTHER SEATS	(FRONT)	ALL SEATS	COMPONENT
ΔV FT/SEC	31	31	26.8	35	30.3
Δt RISE, SEC	0.05	0.06	0.05	0.08	0.08
PEAK g	19	15	16.5	14	12.1
HORIZONTAL	FRONT	OTHER SEATS		ALL SEATS	
ΔV, FT/SEC	42	42		44	
Δt RISE, SEC	0.05	0.06		0.09	
PEAK g	26	21		16	

1.2 PURPOSE

The purpose of this effort is to analyze the effect that airplane size has on the dynamic floor pulse(s) generated within the aircraft cabin, during a crash impact event. The investigation includes:

- A review of narrow-body and wide-body section test results and supporting analytical model results.
- The utilization of the CID validated KRASH model to perform additional parametric studies.
- The definition of relationships between parameters which influence aircraft structure dynamic response.
- The development of airplane preliminary size effect trend curves for cabin floor dynamic pulses in terms of triangular pulse acceleration magnitude, velocity change and pulse duration, which are applicable to a wide range of airplane categories including "commuters."

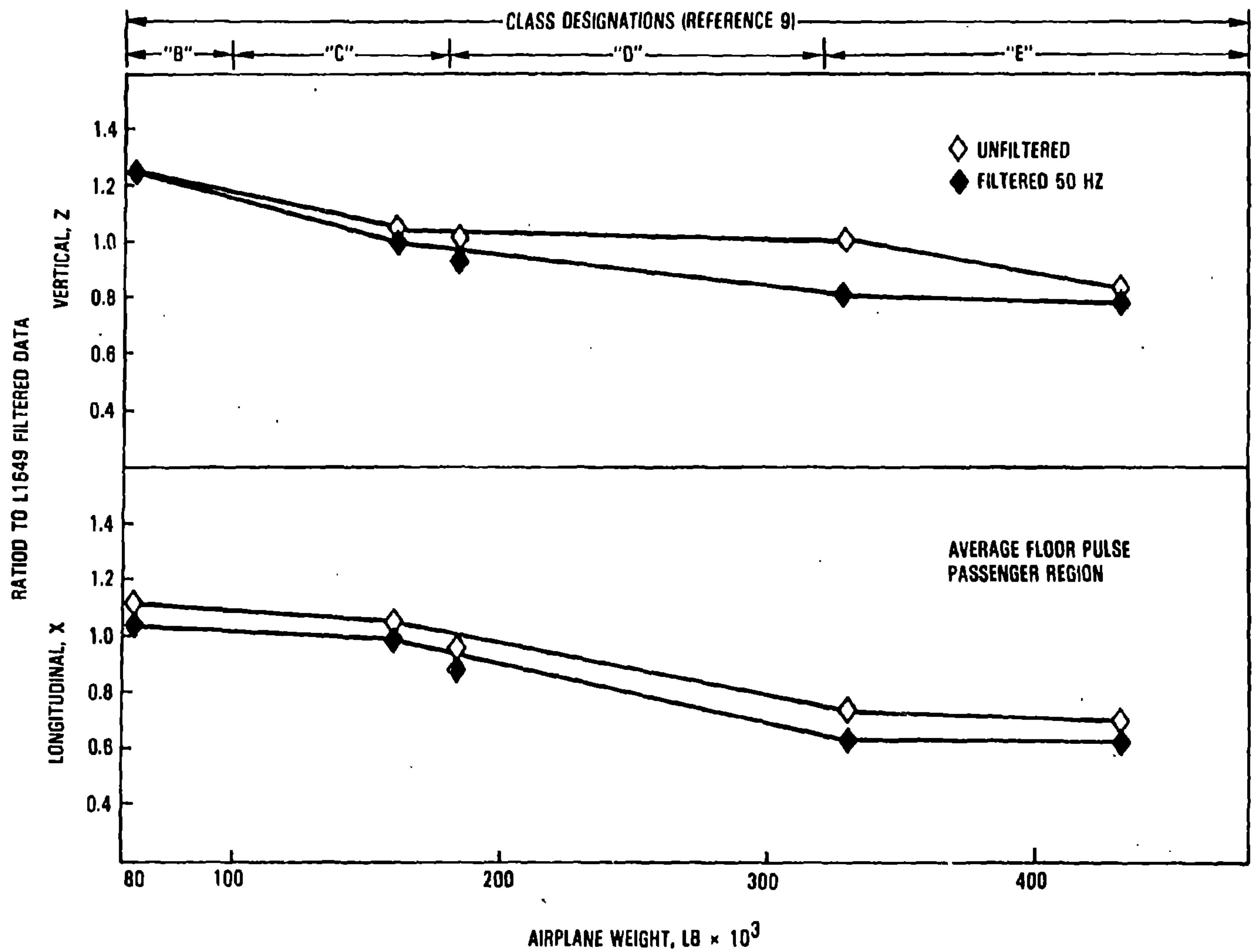

Figure 1. Peak Acceleration Versus Airplane Size and Weight

2. DISCUSSION

2.1 CRASH PULSES

From the study described in reference 9 there are several candidate crash scenarios identified for transport airplanes which should be evaluated. These scenarios are described as follows:

- Ground-to-Ground overrun type accident, such as take-off, abort or landing overrun, which occurs at a low forward speed (40-130 knots), with the landing gears extended and the airplane in a level and symmetrical attitude. The accident occurs on paved runway or hard ground. Damage is sustained by the airplane as it traverses a ditch, road or mound.

- Air-to-Ground hard landing accident, such as touchdown just short of or on the runway. On the average, the sink speed is in the vicinity of 5.2 m/sec (17 ft/sec). Forward velocity is in the range of 126 to 160 knots. The airplane lands with landing gear extended in a nose-up symmetrical attitude ranging from 0° to 14°. These accidents occur on a rigid flat surface with no obstacles or hazards.

- Air-to-Ground impact accident type on hard ground on or off the runway. Sink speed can range up to 10 m/sec (33 ft/sec). Forward velocity is in the range of 126 to 160 knots. Airplane can land with gears retracted or extended in an unsymmetrical attitude. Range of unsymmetry is ±10° for roll and yaw, with pitch attitude variations from 0° to +14°.

The FAA as part of a comprehensive crash dynamics R&D effort (figure 2) quantified cabin floor dynamic pulses for transport category airplanes, as reported in reference 9. The CID full-scale crash test (reference 15), as planned (table 3) with a shallow impact attitude and 17 ft/sec sink speed, is typical of a transport airplane survivable accident. Even the eventual unsymmetrical impact with 13 degrees roll and yaw, as noted in table 3 and depicted in figure 3, is not unrealistic. By contrast, the small light fixed airplanes crash with much steeper attitudes (15° to 45° pitch). A series of four high-wing light airplanes were tested as reported in reference 20. The impact conditions for these tests were selected as representative of the accident history of such small airplanes. The impact conditions are noted in

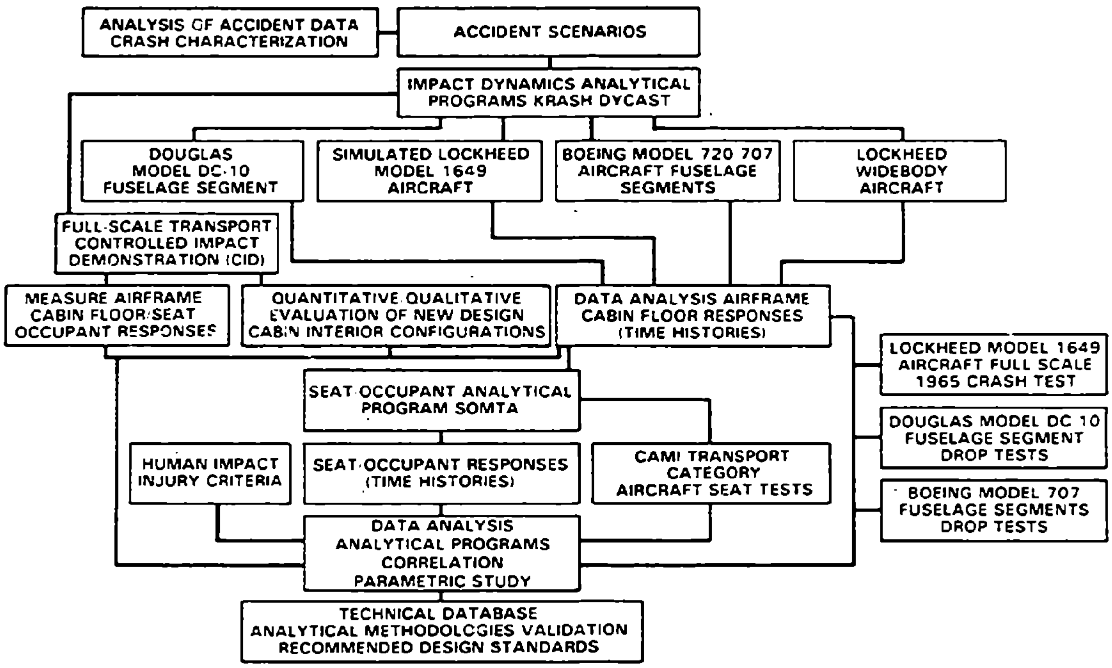

Figure 2. FAA Crash Dynamics Engineering and Development Program

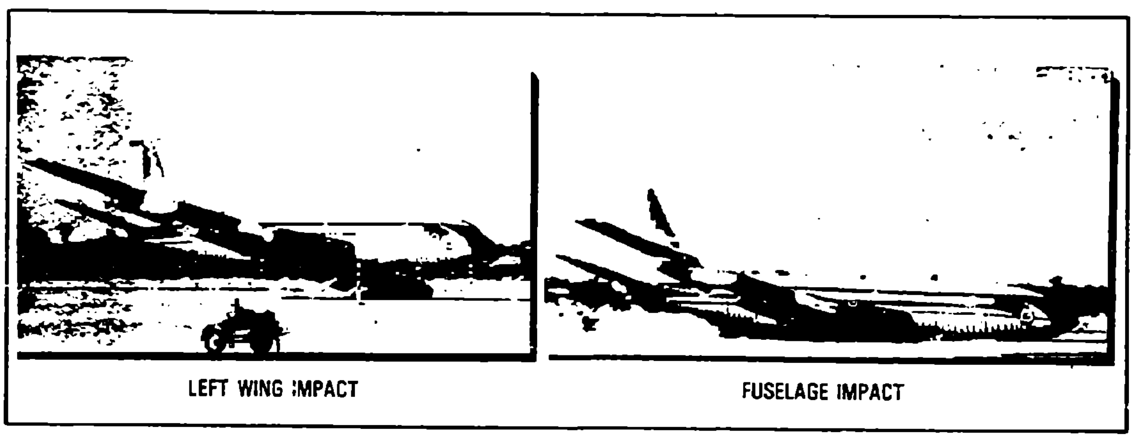

Figure 3. CID Impact Sequence

TABLE 3. COMPARISON OF CID TEST PLANNED AND ACTUAL IMPACT CONDITIONS

	PLANNED	ACTUAL*
SINK RATE, FT/SEC	$17.0\ ^{+3}_{-2}$	17.3
GROSS WEIGHT, LB	175 — 195,000	192,383
GLIDE PATH, DEGREES	3.3 TO 4.0	3.5
ATTITUDE, DEGREES	1 ± 1 (NOSE UP)	0
LONGITUDINAL VELOCITY, KNTS	150 ± 5	151.5
ROLL DEGREES	0 ± 1	−13**
YAW DEGREES	0 ± 1	−13***

*IMPACTED ON LEFT WING OUTBOARD ENGINE. INITIAL CONTACT ON FUSELAGE WAS AT FOLLOWING CONDITIONS: 14 FT/SEC SINK SPEED, NOSE-DOWN ATTITUDE (0.−2.0 DEGREES), FORWARD VELOCITY 150 KNTS CONTACTED FUSELAGE (BS 360 — 460) REGION.

**LEFT WING DOWN
***NOSE LEFT

table 4 and depicted in figure 4. While the accident impact environments differ between small and large airplanes, each has a characteristic pulse that is experienced by the aircraft structure and occupants. For impacts into rigid terrain (air-to-ground) without obstacles (buildings, hillsides, mounds) present, the primary pulse, if there is a significant sink speed involved, is vertical. The major longitudinal pulse in this type of accident is a function of the ground coefficient of friction. On concrete this longitudinal pulse is generally lower in magnitude than the vertical pulse but of the same duration. The vertical pulse is critical to occupants because it is a major contributor to spinal injuries. The actual pulse magnitude and shape that the occupant is exposed to is directly related to the fuselage underside crush, seat stroke and landing gear stroke (if extended). In general, the fuselage underside crush is the dominant parameter necessary to reduce the vertical velocity to zero from the initial sink speed.

TABLE 4. SUMMARY OF HIGH-WING LIGHT AIRPLANE CRASH TEST IMPACT CONDITIONS

	TEST NUMBER			
	1	2	3	4
IMPACT VELOCITIES (MPH)				
ALONG FLIGHT PATH	55.5	50.8	58.1	55.9
LONGITUDINAL	47.4	48.6	47.6	48.4
VERTICAL	28.7	14.8	33.2	31.9
ANGLES (DEGREES)				
FLIGHT PATH (γ)	− 30.72	− 17.	− 34.86	− 32.
IMPACT (θ)	− 30.17	13.5	− 39.4	− 34.8
ATTACK (α)	0.57	+ 30.5	− 4.54	− 2.8
ROLL(ϕ)	+ 4.13	+ 3.25	+ 18.75	< 1.0
YAW (ψ)	− 3.27	− 11.5	− 7.9	< 1.0
ROTATIONAL VELOCITIES (DEG/SEC)				
PITCH ($\dot{\theta}$)	46.4	6.9	14.3	18.2
ROLL ($\dot{\phi}$)	NEGLIGIBLE	NEGLIGIBLE	NEGLIGIBLE	NEGLIGIBLE
YAW ($\dot{\psi}$)	NEGLIGIBLE	NEGLIGIBLE	NEGLIGIBLE	NEGLIGIBLE

γ IS NEGATIVE IN DIVE
$\theta, \dot{\theta}$ ARE POSITIVE NOSE UP RELATIVE TO GROUND
α IS POSITIVE NOSE UP RELATIVE TO FLIGHT PATH
$\phi, \dot{\phi}$ ARE POSITIVE RIGHT WING DOWN
$\psi, \dot{\psi}$ ARE POSITIVE TAIL LEFT
AND $\theta = \gamma + \alpha$
FT/SEC = 1.467 X MPH

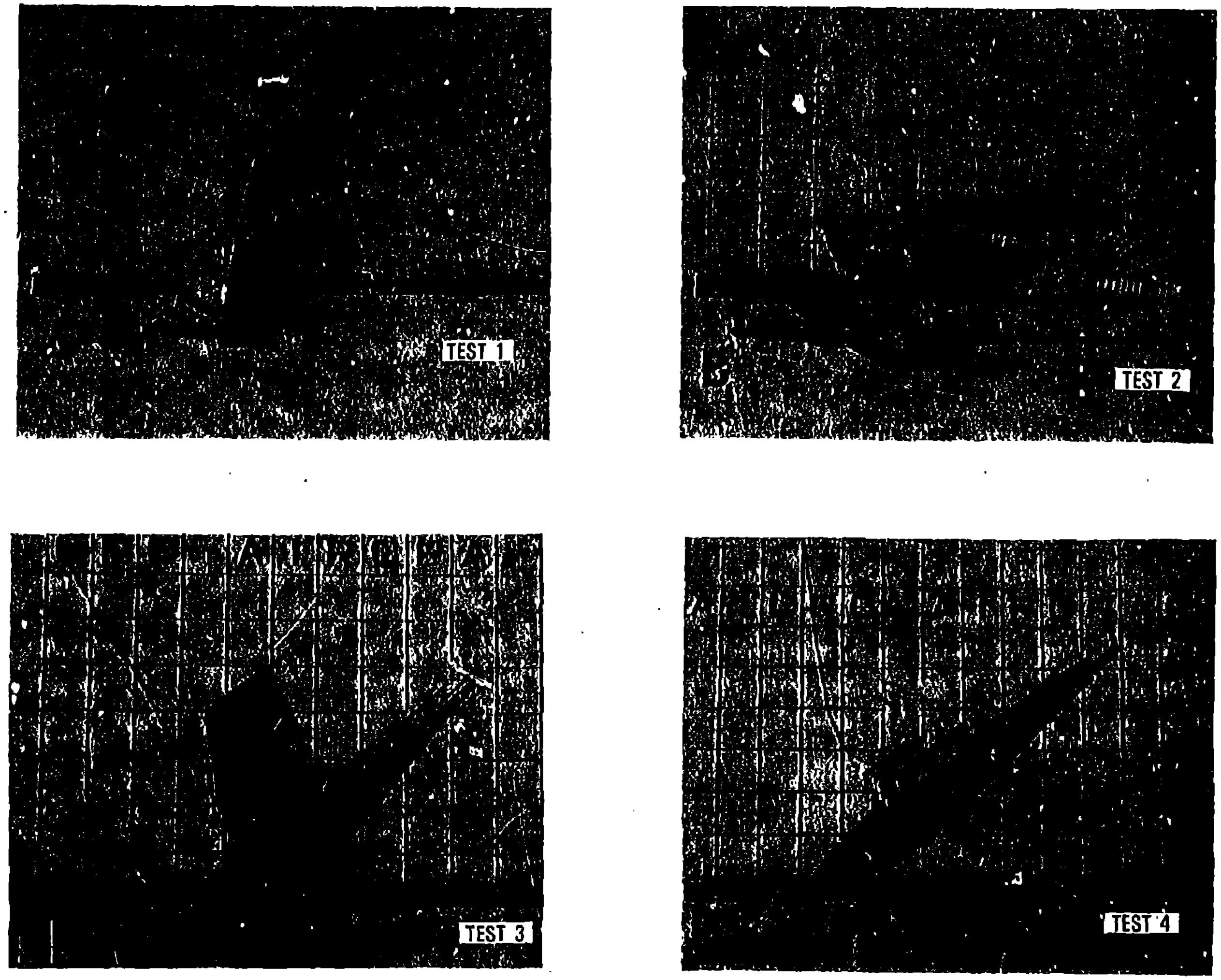

Figure 4. Initial Impact Position of High-Wing, Single-Engine Airplane Crash Tests

For airplanes to develop a significantly high longitudinal pulse during a survivable accident there must be a collision with a major obstacle or an impact into a sloped terrain after the initial air-to-ground contact. The L1649 full-scale crash test results (reference 19) illustrate an impact onto a 20 degree slope which resulted in fuselage breakup and some fairly significant longitudinal pulses. However, as stated, smaller airplanes generally crash into the ground with steeper impact angles than do the large transport airplanes. The test of high-wing airplanes with 30 degree impact angles show increased longitudinal pulses versus those associated with the lower attitude CID test even though the latter occurred with a much higher initial forward velocity. The impact forces developed in the airplane's principal axes are significant for assessing occupant injury potential. The steeper the impact angle the higher the forces in the airplane fore-aft direction. On concrete there is a significant slide-out which accounts for much of the longitudinal velocity reduction. In soft dirt, the longitudinal motion is arrested in a shorter time and slide-out distance and therefore fuselage structural crush in the fore-aft direction plays an important part in shaping the pulse experienced by the occupants. The post-impact consequences of the four high-wing light airplane crash tests are shown in figure 5. As can be noted the nose-down impacts (tests 1 and 3) on concrete are not nearly as dangerous to the occupants as the nose-down impact (test 4) into dirt. The latter developed significantly higher airplane longitudinal forces. The longitudinal pulse can influence spinal injuries if it occurs simultaneously with a vertical pulse. However, the more significant injury that can occur due to primary longitudinal forces is associated with a head impact into the surrounding cabin structure, particularly with only lap belt restraints. Other injuries associated with high longitudinal forces are due to excessive lap belt loads and occupant flailing.

The following discussions in this section address vertical-only and longitudinal-only pulses as they relate to the fuselage's ability to crush, whether it be underfloor deformation (vertical impact) or forward fuselage deformation (longitudinal impact).

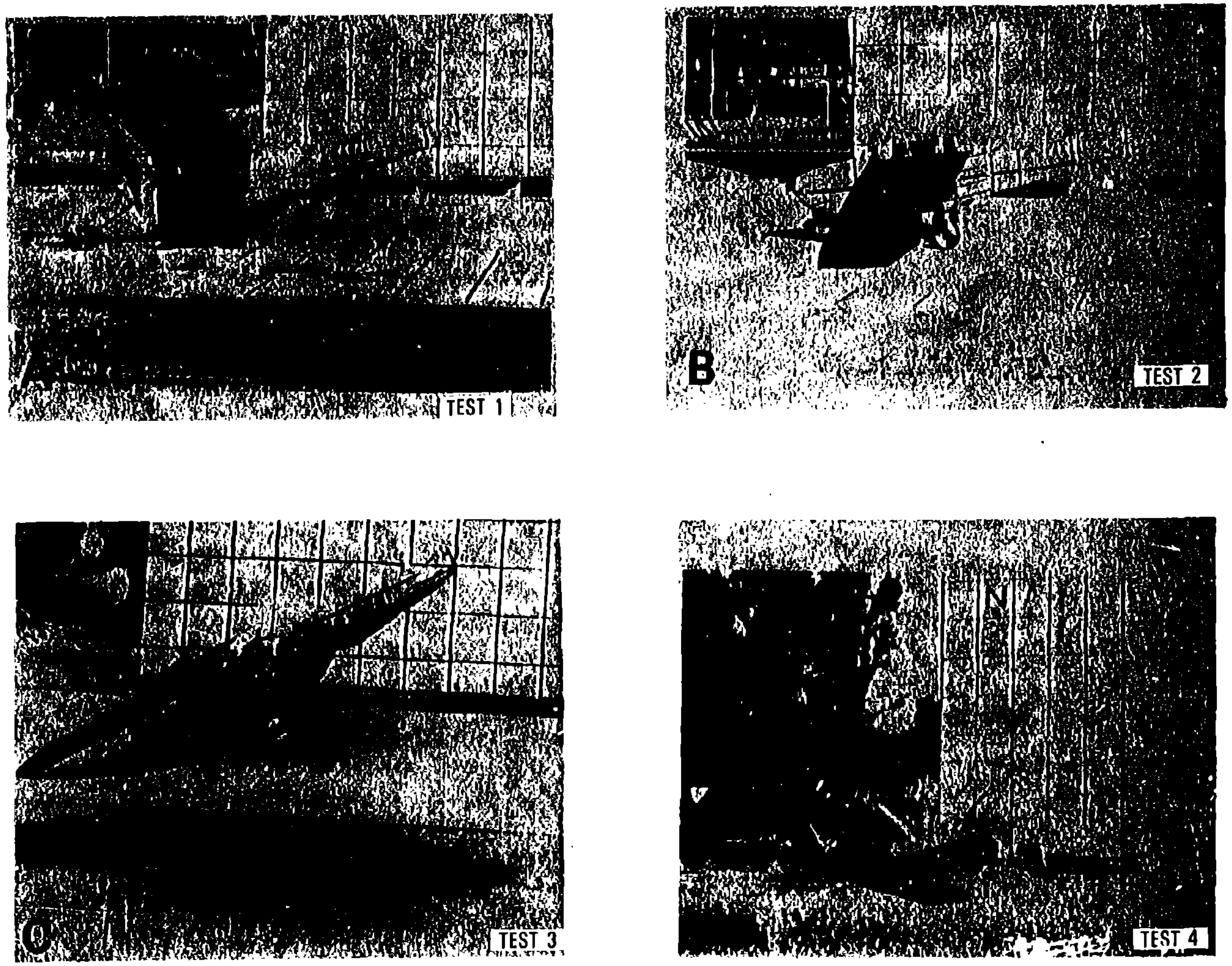

Figure 5. Post-Impact Views of High-Wing, Single-Engine Crash Tests

2.2 VERTICAL DIRECTION

The following simplified approximate expression relates aircraft fuselage crush energy dissipation and kinetic energy to be absorbed:

$$\frac{1}{2}\ \frac{W}{g}V^2 + W\delta = WG_z\delta .$$

$$V^2 = 2g(G_z\,\delta - \delta) = 2g\delta(G_z - 1)$$

$$\Delta V = 19.6\ \sqrt{2\delta(G_z - 1)}$$

$$\Delta V = 19.6\ \sqrt{2\delta(\frac{G}{2}\ p-1)} = 19.6\sqrt{\delta(G_p-2)}$$

where V = velocity change, inch/second

δ = aircraft fuselage crush, inch

G_z = constant average vertical load factor

G_p = peak acceleration (based on a triangular pulse of equal duration to achieve same ΔV)

g = 386.4 in/sec/sec

The vertical velocity-crush distance-peak acceleration triangular pulse relationship is plotted in figure 6. The relationship plotted in figure 6 is based on the final velocity being zero, which is usually the case for the vertical direction. Table 5 presents representative airplane sizes and weight characteristics obtained from reference 9. Included in table 5 are approximate underfloor available crush distances. Table 6 provides approximate strength relationships along with crush potential for the various airplane categories. The estimated crush range for various airplane sizes for categories are illustrated in figure 6 along with additional data such as:

- Narrow-body airplane section test results (references 10, 11, 12)
- Wide-body airplane frame section test results (references 13 and 14)

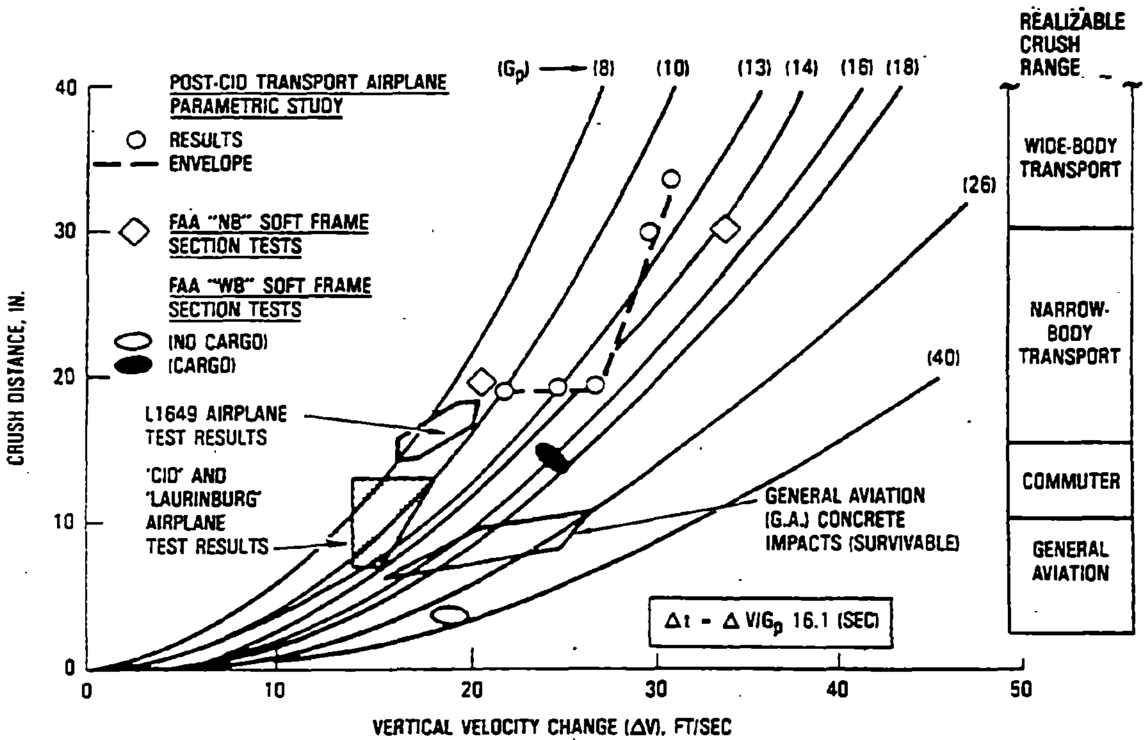

Figure 6. Crash-Velocity Change - Peak Acceleration Relationship, Vertical Direction

- "CID," "Laurinburg," and L1649 full-scale airplane test results (references 15, 16, 19)
- Transport airplane parametric sensitivity study data (reference 18)
- General aviation airplane test results (references 20, 21, 22)

The parametric study results (reference 18) were based on the CID airplane which had a takeoff weight of 195,000 pounds. The results of that study are considered appropriate for the mid-size narrow-body airplane category. The parametric study shows that as additional crush is allowed to achieve a higher impact velocity capability, the "g" level reduces and the

TABLE 5. AIRPLANE SIZE AND WEIGHT CHARACTERISTICS

CATEGORY	AIRPLANE CLASS	MAXIMUM DESIGN TAKEOFF WEIGHT (lb)	NOMINAL RANGE NO. PASSENGERS	FUSELAGE OVERALL LENTH (in.)	FUSELAGE CRUSH PARAMETERS		
					DIAMETER (in.)	LENGTH (in.)	AVAILABLE BELOW FLOOR DISTANCE (in.)
FAR 23	NORMAL (GENERAL AVIATION)	12,500	1 – 9	90 – 128	48 – 60	60 – 80	4 – 12
FAR 23	COMMUTER	12,500 – 19,000	10 – 19	120 – 720	84 – 96	80 – 480	6 – 15
FAR 25	CLASS B *	19,000 – 125,000	50 – 80	900 – 1,118	120 – 132	600 – 750	16 – 40
FAR 25	CLASS C *	125,000 – 200,000	90 – 115	1,200 – 1,800	144 – 168	800 – 1,200	40 – 84
FAR 25	CLASS D *	175,000 – 300,000	115 – 363 **	1,644 – 2,112 **	168 – 216 **	1,400 – 1,400 **	84 – 108 **
FAR 25	CLASS E *	420,000 – 785,000	250 – 500	2,160 – 2,772	224 – 264	1,400 – 1,860	108 – 120

* REFERENCE 9 DESIGNATION
** INCLUDES 2 WIDEBODY AIRPLANES (B767, A300)

TABLE 6. AIRPLANE CATEGORY CRUSH AND STRENGTH CHARACTERISTICS

CATEGORY	AIRPLANE CLASS	MAXIMUM DESIGN TAKEOFF WEIGHT (LB)	REPRESENTATIVE FUSELAGE CRUSH SPACE				PER UNIT LOAD FACTOR (N_z = 1)		FUSELAGE SHELL		STRENGTH FACTOR *	
			DEPTH (INCH)	WIDTH (INCH)	LENGTH (INCH)	VOLUME $IN.^3 \times 10^3$	$\frac{WT \cdot N_z}{CRUSH\ SURFACE}$ (LB/IN^2)	$\frac{WT \cdot N_z}{CRUSH\ VOLUME}$ (LB/IN^3) $\times 10^3$	DIAMETER (INCH)	THICKNESS (INCH)	SHEAR FACTOR S_z	BENDING FACTOR M_y
FAR 23	GENERAL AVIATION	12,500	6	20	60	7.2	10.4	1.7	60	–	–	–
FAR 23	COMMUTER	19,000	12	33	100	39.6	6.1	0.50	100	0.035	–	–
FAR 25	SMALL NARROW-BODY	125,000	20	48	800	768	3.3	0.16	144	0.043	0.72	0.62
FAR 25	MID-SIZE NARROW-BODY	235,000	25	56	1200	1680	3.5	0.14	168	0.051	1.00	1.00
FAR 25	WIDE-BODY	430,000	35	75	1600	4200	3.6	0.10	224	0.071	1.85	2.47

*NORMALIZED TO MID-SIZE NARROW-BODY AIRPLANE CONFIGURATION; $S_z = f(rt)$, $M_y = f(r^2 t)$

time duration increases. The analysis presented in reference 18 assumes that the fuselage underside crush is nearly constant until the structure "bottoms-out." The uniformity of the crush load is one measure of efficiency with regard to energy absorption. However, this connotation of efficiency is not to be confused with the efficiency related to the utilization of available crush distance.

For the narrow-body airplane configuration studied in reference 18, 24 inches of frame crush is assumed available in the aft fuselage region. This amount of crush is considerably less than the total available below passenger floor depth of 85 inches. Consequently less crush produces either a higher peak acceleration (G_z), or a lower velocity change (ΔV) for the same peak acceleration magnitude. The crush distances for the narrow-body and wide-body airplanes are estimated for the purpose of this discussion by the ratio of the available below floor depths using the CID airplane as the typical mid-range narrow-body airplane. For the larger transports, the hard structure in the wing center section would not be expected to crush as much as the soft frames. However, the data in figure 6 is based on the premise of a uniform force and average crush throughout the entire fuselage.

As part of the overall FAA crash dynamics program several frame section vertical impact tests were conducted. From these tests, data such as impact velocity, crush and acceleration were obtained. The frame sections tested are representative of an airplane in the 200,000 pound to 300,000 pound MTOW range. The CID test specimen, which is of similar size and fuselage structure construction, is representative of an airplane in the 190,000 pound to 235,000 pound Maximum Design Takeoff Weight range. The L1649 airplane test specimen, which provided substantial pulse test data, weighed 159,000 pounds and thus, is also representative of a mid-range narrow-body airplane.

The results of the frame section drop tests provide some insight into airframe behavior. Two of the tests (references 10 and 11) were performed with narrow-body airplane sections (with and without lower compartment cargo luggage) and each at an impact velocity of 20 feet/second. The test results are noted in figures 7 and 8 for the test with (NB1) and without cargo (NB2), respectively. The generated floor acceleration responses were comparable. The failure of each lower fuselage reflected the effect of the cargo (or lack of cargo) as noted in the formation of a cusp at the lower extremity. The "cargo version" specimen weighed 6440 pounds and experienced a floor average vertical load factor (G_z) and lower fuselage crush of approximately 5.0g and 18 inches, respectively. This result is noted in figure 6. Another FAA test of a similar constructed fuselage section weighing 8883 pounds with cargo, was performed at an impact velocity of ≈ 35 feet/second (reference 12). This specimen floor experienced an average vertical load factor (G_z) of approximately 7.0g and a crush of 27 inches, respectively. This data point is also plotted on figure 6. However, this latter data point was generated from a "soft" fuselage structure section without end restraints such as those associated with bulkhead or wing center section hard points. The parametric study results (reference 18) showed that fuselage crush for a complete airplane can be limited depending on the impact attitude and the location of hard point structure. Therefore, drop tests of a fuselage section(s) that contained bulkheads or wing center section hard points would produce a higher vertical acceleration response and show significantly less lower fuselage crush.

When one examines results presented in references 11 and 12 in terms of the ratio of load to crush volume, the following is obtained:

- <u>Reference 11</u> (V_i = 20 feet/second, weight = 6440 pounds)

  $G_z \sim 5.0g$

  Crush volume $\sim 20 \times 45 \times 120 = 108{,}000 \text{ in}^3$

  $\frac{\text{pound}}{\text{in}^3} \sim .30$

ORIGINAL PAGE IS
OF POOR QUALITY

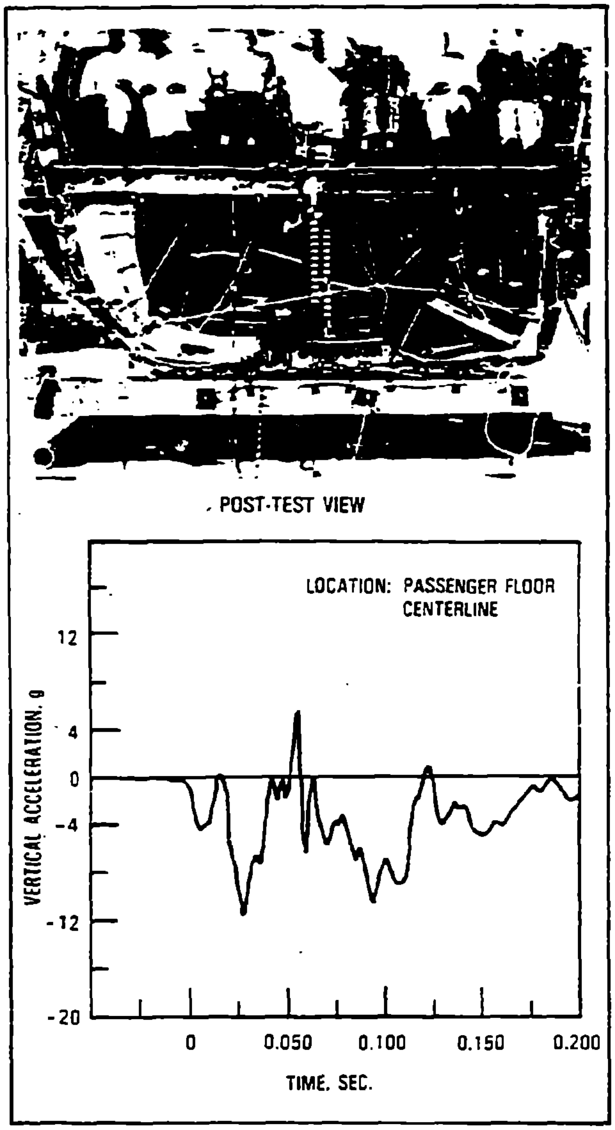

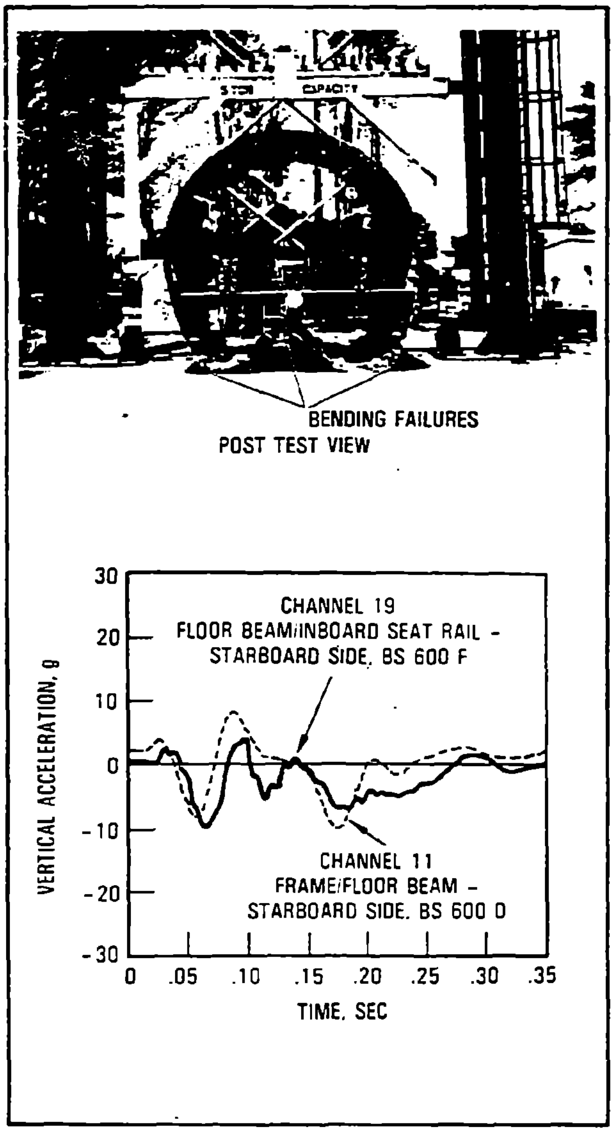

Figure 7. Results of Narrow-Body Airplane Forward Fuselage Section Test (with Cargo) (Reference 10)

Figure 8. Results of Narrow-Body Airplane Forward Fuselage Section Test (without Cargo) (Reference 11)

- Reference 12 (V_i = 35 feet/second, weight = 8883 pound)

  $G_z \sim 7.0g$

  crush volume 27 x 50 x 120 = 144,000 in^3

  $\frac{pound}{in^3} \sim .37$

From table 6, the "pound/inch^3" parameter for a 235,000 pound GTOW mid-size narrow-body transport airplane and a G_z = 6.5 should be approximately 1.04. The table 6 data for this airplane category is based on 235,000 pounds acting over 1200 inches or 200 pounds/inches, although in reality a large percentage of the weight associated with the wing and fuel is concentrated nearer to the wing-center and main landing gear sections. The section tests are based on weight loading distributions, of ~ 54 pounds/inch and 74 pounds/inch. Thus, for a comparable weight/length loading, the reference 11 and 12 results would be 1.1 and 1.0, respectively. The static strength of the overall floor and supporting structure for large transport category airplanes is probably in the range of G_z = 4.5g to 6.5g (down). Locally, the structure probably can resist higher loads. A structure experiences dynamic loads during a crash condition. The associated accelerations could be higher than the static load factors.

The FAA conducted two wide-body section tests; one (WB1) without cargo (5000 lb) and the other (WB2) with cargo (10800 lb). The tests were conducted at impacts of 20 ft/sec and 25 ft/sec, respectively. The latter widebody test included approximately 5100 lb in containers on the cargo floor. The post-test crush of the fuselage underside for both these tests are shown in figure 9. Table 7 presents the test parameters for the two aforementioned wide-body airframe sections, as well as the two 20 feet/second impacts narrow-body airframe impact tests (references 10 and 11), which were discussed earlier. A comparison is shown of the data in table 8. Since all specimens are the same length, the crash data presented in table 8 is normalized to a unit length by dividing by 120. Table 8 contains the following information:

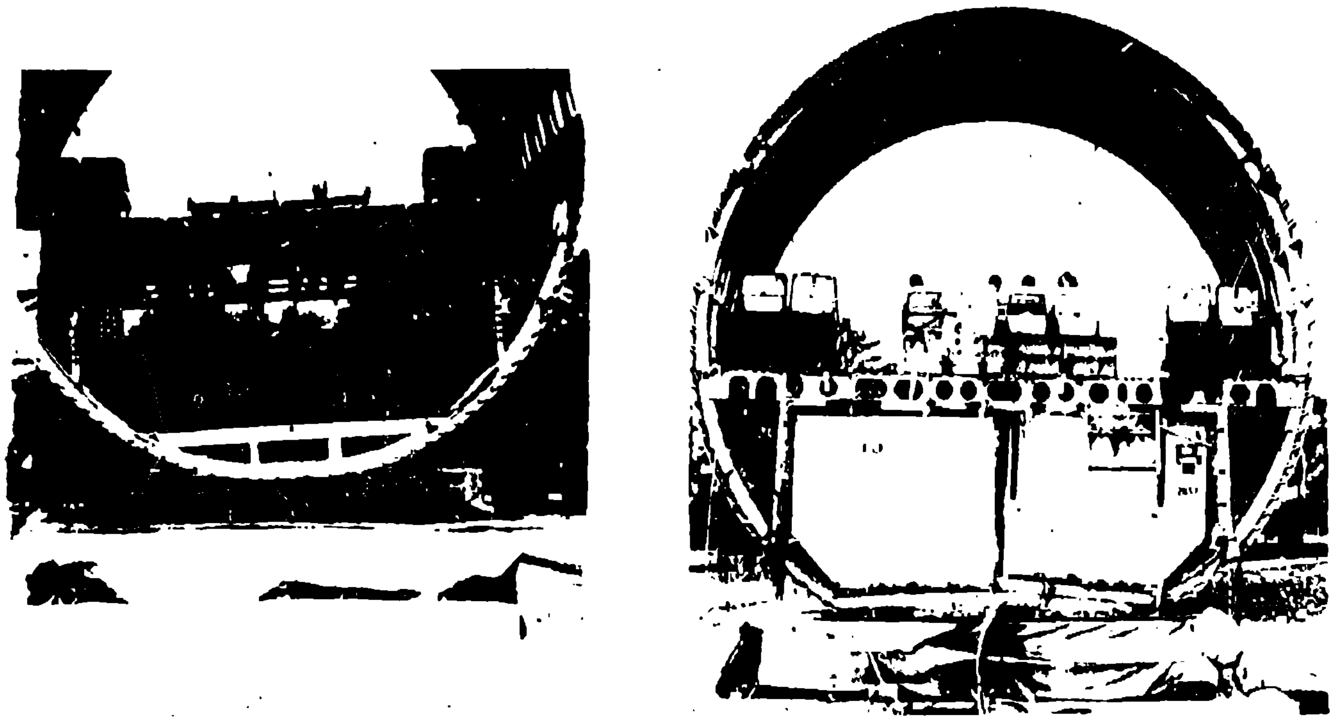

(a) LIGHTLY LOADED SECTION: 20 FT/SEC IMPACT VELOCITY

(b) HEAVILY LOADED SECTION: 25 FT/SEC IMPACT VELOCITY

Figure 9. Wide-Body Frame Sections Post-Test Results

TABLE 7. FAA/NASA FULL-SCALE SECTION IMPACT TESTS

STRUCTURE	APPROXIMATE* WEIGHT (lb)	AIRPLANE	TEST PERFORMED BY	IMPACT FT/SEC	CRUSH DISTANCE – INCHES STATIC AT REST
FORWARD FUSELAGE	5100	NARROW-BODY	NASA	20	14 – 16
FORWARD FUSELAGE	6400	NARROW-BODY	FAA	20	17 – 20
AFT FUSELAGE	5000	WIDE-BODY	FAA	20	1 – 2
AFT FUSELAGE	10800	WIDE-BODY	FAA	25	11 – 15

TABLE 8. COMPARISON OF SECTION AND TEST PARAMETERS

(C1) CONFIGURATION AND WEIGHT (LB)	(C2) POTENTIALLY REALIZABLE DEPTH x WIDTH (IN) (IN)	(C3) = COLUMNS (C1)/(C2)	(C4) PASSENGER FLOOR LOAD/WIDTH (LB)/(IN) **	(C5) KINETIC ENERGY FT-LB @ 20 FT/SEC	(C6) APPROX. CRUSH AREA ACHIEVED (DEPTH x WIDTH) (IN) (IN)	(C7) RATIO OF ENERGY TO CRUSH AREA (C5)/(C6)	(C8) CRUSH AREA UTILIZATION EFFICIENCY (C2)/(C6)
NB1 – 5100	25 x 56	3.6	2700/140 - 30.5	31677	16 x 40	7128	45.7
NB2 – 6400	25 x 56	4.6	2700/140 - 30.5	39751	18 x 45	7050	57.8
WB1 – 5000	35 x 75	1.9	2400/200 - 12.0	31055	2 x 50	44790	3.7
WB2 – 10800	35 x 75	4.1	2700/200 - 15.5	104809*	13 x 100	11612	49.5
WB2 – 5100 (CARGO FLOOR ONLY)	13 x 100	3.9	5100/100 - 51.0	49495*	13 x 100	5483	100

NB - NARROW-BODY AIRFRAME SECTION

**LOAD INCLUDES OCCUPANT AND FLOOR WEIGHTS

WB - WIDE-BODY AIRFRAME SECTION

* - BASED ON 25 FT/SEC

a. configuration and weight - column 1

b. potentially realizable crushable area (width and depth) - column 2

c. ratio of weight divided by the width x depth parameter - column 3

d. passenger floor load (weight)/width - column 4

e. kinetic energy (ft-lb) to be dissipated at 20 ft/sec (25 ft/sec for the heavier loaded wide-body section) - column 5

f. approximate crushable area (width x depth) achieved during the test - column 6

g. energy/crushable area achieved - column 7

h. efficiency of utilization of available crush area - column 8

Figure 10 plots peak acceleration at the passenger cabin floor versus triangular pulse base duration for the two narrow-body (NB1, NB2) and two wide-body, (WB1, WB2) airframe section tests. The data in figure 10 shows that the lightly loaded wide-body airplane section produces relatively high peak g's, but with short durations. The heavier loaded wide-body airplane section produced dramatically reduced floor peak g's and increased time

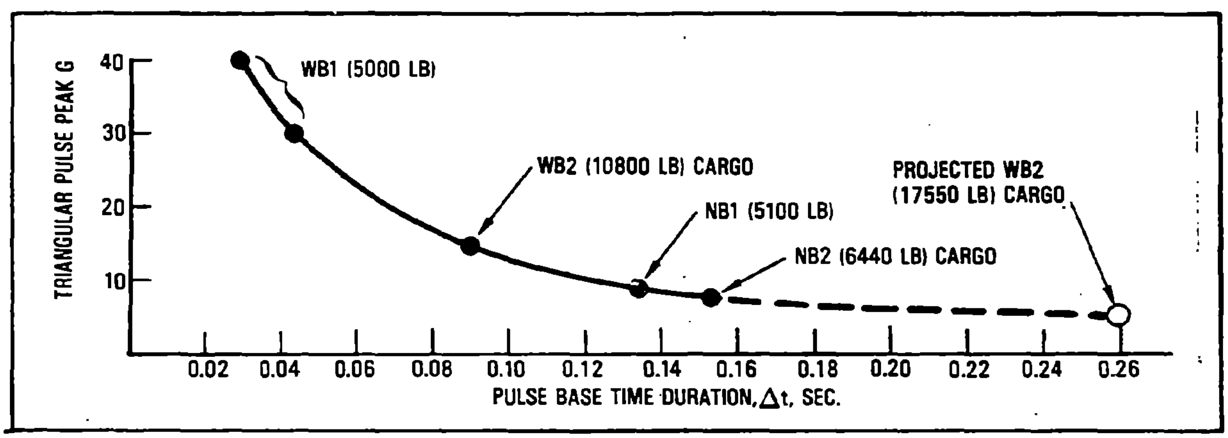

Figure 10. Passenger Floor Response Pulse

durations when compared to the lightly loaded wide-body section test. However, the wide-body section test results still show higher g's and shorter time durations (Δt) than the narrow-body section test results. In order to assess the differences between the narrow-body and wide-body section floor response g's, the data in table 8 were reviewed and plotted in figures 11, 12 and 13. From figure 11, it can be observed that the weight and, consequently the associated kinetic energy, for the WB1 test was extremely low relative to the available crush. Comparisons of test results for the NB1, NB2, and WB2 sections show that the weight to available crush ratio is relatively close. figure 12 suggests that the passenger floor for the wide-body is substantially less densely loaded than the narrow-body sections. Figure 13 shows both the ratio of energy absorbed to actual crush area as well as the efficiency of utilization of the available crush. The kinetic energy to crush area ratios come from column 7 in table 8. The efficiency of utilization of the available crush term is defined in column 8 of table 8. As can be observed in figure 13 the slopes range in values from 44790 to 5483 (kinetic energy-to-crush area), while the corresponding efficiencies range from 3.7% to 100%. Figure 13 also indicates that the WB2 test produced about the same ratio of kinetic energy to actual crush area as the two narrow-body section tests. The lower slope appears to correspond to the higher efficiency. Also the lower slope and higher efficiency would appear more desirable since it requires more crush to occur, which generally is accompanied by lower peak accelerations and longer pulse time durations. Since in the heavier loaded wide-body section test (WB2), the cargo floor crushed to its maximum available space, it comes close to 100% utilization of its available structural crush area. It would appear in the WB2 test that for the lower fuselage to experience structural crush in excess of the below-cargo floor available distance (13 inches), the passenger floor would have to be more heavily loaded and/or the impact velocity would have to be higher. The higher weight/velocity condition would have to result in crushing of the fuselage frames above the cargo floor. Based on the plotted results shown in figure 13, it would appear that the increased loading and/or velocity would result in a slope (efficiency) somewhere between 11612 (49.5%) and 5483 (100%). The narrow-body airplane sections exhibited a crush area utilization ratio of between 7050 and 7128. Thus, as an initial goal it

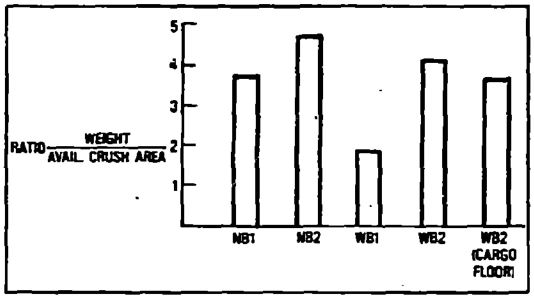

Figure 11. Section Weight-to-Available Crush Ratio Versus Test Configuration

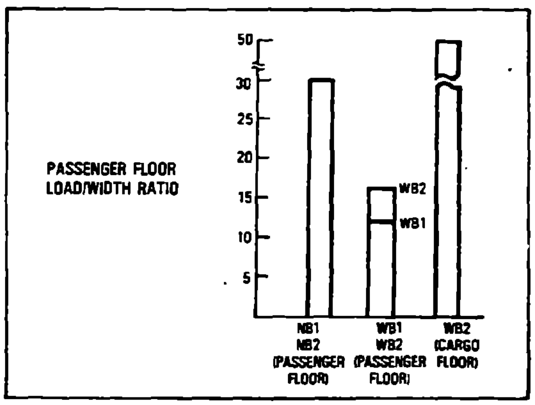

Figure 12. Passenger Floor Loading Versus Test Configuration

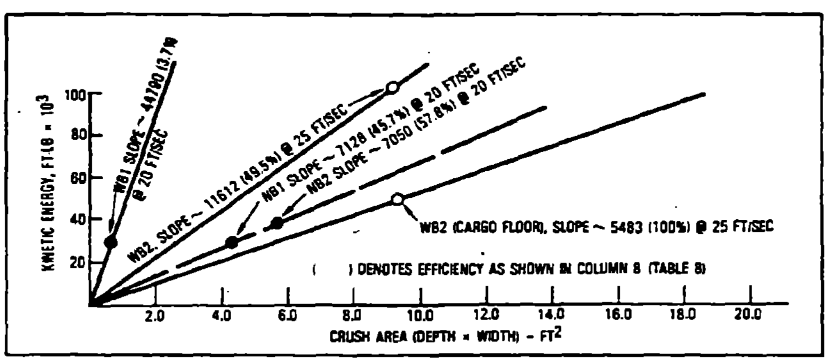

Figure 13. Kinetic Energy Versus Crush Area

would appear desirable for the wide-body airplane section tests to achieve approximately the same ratio, while maintaining an efficiency rating of at least 50%. This approach assumes that the additional passenger floor loadings are transmitted through to the lower fuselage frames and will produce some plastic hinges as was noted in the narrow-body frames. The wide-body airplane passenger floor posts, which are also a load path to the lower frame, would have to be evaluated for possible failure and subsequent load path change.

Assuming one could hold this ratio to around 7200 for the wide-body section, as was the case for both the narrow-body tests additional frame failure and crush beyond that of the cargo floor would have to occur in order to lower the passenger floor g's. Based on figure 12 data, a 2.5 fold increase in passenger floor loading could make the narrow-body and wide-body tests comparable in loading. Following this reasoning and using the 25 ft/sec impact wide-body section test data then:

1. additional passenger floor weight = 2700 lb. x 2.5 = 6750 lb.
2. total weight = 10800 lb + 6750 lb = 17550 lb
3. kinetic energy = $104809 \times \frac{17550}{10800} = 170315$ ft.-lb.
4. energy/crush area = 7200 (select as goal since it was achieved in NB tests.)
5. crush area = $\frac{(3)}{(4)} = \frac{170315}{7200} = 23.65\ ft^2 = 3406\ in^2$
6. approximate crush <u>depth</u> and <u>width</u> required = 40 in. x 85 in. = 3400 in.^{2}
7. peak g in triangular pulse [K.Energy = weight.depth.$\frac{\text{peak g}}{2}$] = $\frac{170315\ (2)}{(17550)(3.3)}$ 5.9
8. triangular pulse base duration, $\Delta t = \frac{(25)(2)}{(G_p)(32.2)}$ .26 seconds [$\Delta V = (1/2)(G_p)(32.2)(\Delta t)$]

This hypothetical pulse is projected on the curve shown in figure 10. The above approach assumes the additional passenger floor loadings is transmitted through to the lower fuselage frame and will produce some plastic hinges as was noted in the narrow-body frames. The floor posts, which are also a load path to the lower frame, would have to be considered for possible failure and subsequent load path change. The crush areas are estimates based on approximate averages of depth and width. A detailed evaluation of the cross-sectional area of a segment as a function of depth would provide more accurate numbers.

2.3 LONGITUDINAL DIRECTION

The crush-velocity change - acceleration response relationships, along with supporting analysis and test data presented in figure 6 is oriented toward vertical pulses. A similar relationship which exists for the longitudinal-direction pulse is shown in figure 14. Included in figure 14 are data from general aviation airplane tests (references 20-22), a narrow-body transport airplane test (reference 19) as well as the data from a parametric sensitivity study (reference 18). As noted for the longitudinal direction pulses, the relationship shown in figure 14 is also based on a final velocity being zero. In some instances the primary longitudinal pulse occurs simultaneously with the primary vertical pulse and the final longitudinal direction velocity does not reach zero until after a lengthy slideout. In this situation the crush distance may not be consistent with the peak acceleration and velocity change data, since the latter are likely to have been obtained from test data.

As noted earlier, the parametric sensitivity study results (reference 18) show that as the crush increases, the potential for a higher velocity change exists. However, the increased crush and higher velocity change generally occurs with a decrease in acceleration magnitude. The general aviation tests reported in references 20 and 21 provide comparisons of two nearly identical high-wing airplane impacts with the major difference being in the impact terrain (concrete and soil). Both tests were performed with a flight path velocity of approximately 82 feet/second. Appendix B contains details of

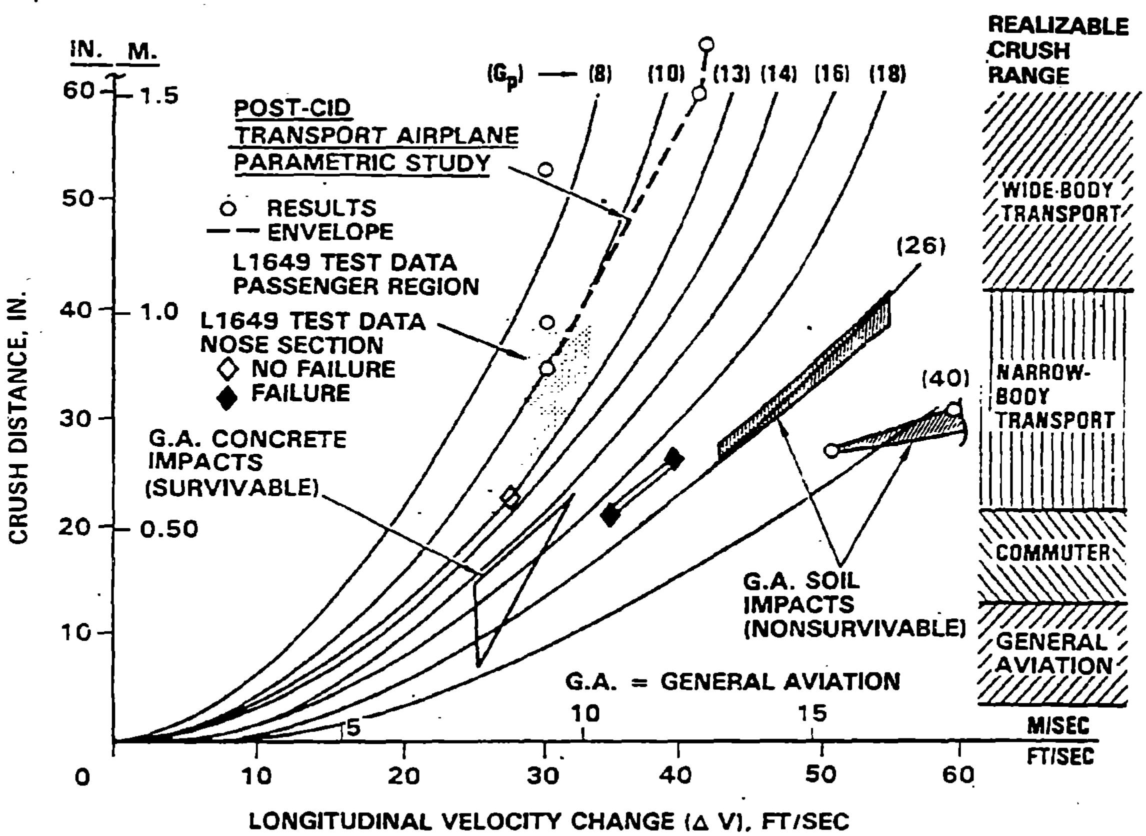

Figure 14. Crush-Velocity Change - Peak Acceleration Relationship, Longitudinal Direction

these test results. Reference 22 also provides comparative data for two nearly identical impacts for a single-engine low-wing general aviation airplane. The impact onto concrete produces a primary longitudinal pulse in the proximity of the pilot and copilot of peak acceleration levels between 17 g's to 30 g's and a velocity change of approximately 24 ft/sec to 32 ft/sec. While the damage is severe, particularly in the forward fuselage, the condition is considered survivable. The impact onto soil devastates the airplane forward fuselage structure and occupiable cabin region and is considered nonsurvivable. This impact produces a primary longitudinal pulse of approximately 25 g's to 50 g's peak acceleration and a velocity change of 38 ft/sec to 60 ft/sec. The data from the parametric study and the general aviation airplane tests onto soil are based on final longitudinal velocities equal to zero, so the crush distances are consistent with the peak g's and velocity changes depicted in figure 14.

As can be observed in comparing figure 14 in contrast to figure 6, there is much less test data available for the longitudinal direction pulse. However, the two general aviation airplane crash tests involving soil terrain provide data in which the longitudinal forces are extremely high and the impact situation is considered nonsurvivable. Crush distance in the case of longitudinal forces, represents either the amount of deformation experienced in the forward fuselage due to a "head-on" impact, into a wall or an effective longitudinal distance associated with a combined directional loading impact. In the case of a "head-on" impact the magnitude of the acceleration forces tend to decrease the further the location from the impact region, provided crush is available. Typically this accident could be nonsurvivable in the forward cabin and survivable in the aft cabin. Thus, the use of longitudinal crush distance as a parameter is more difficult to identify when compared to the vertical impact condition. However, to a degree the fore-aft crush region can be considered proportional to the vertical crush distance based on airplane category.

3. SUMMARY OF RESULTS

Figures 15 and 16 show the size trend curves for the vertical and longitudinal directions, respectively. On the basis of a mid-crush region for each respective airplane category the applicable range of floor dynamic pulses are developed and shown in table 9. The vertical pulse trend range is based on enveloping all the measured and analytically developed data points except for one narrow-body section drop test point. This point is not considered applicable for reasons discussed in the previous section. The longitudinal

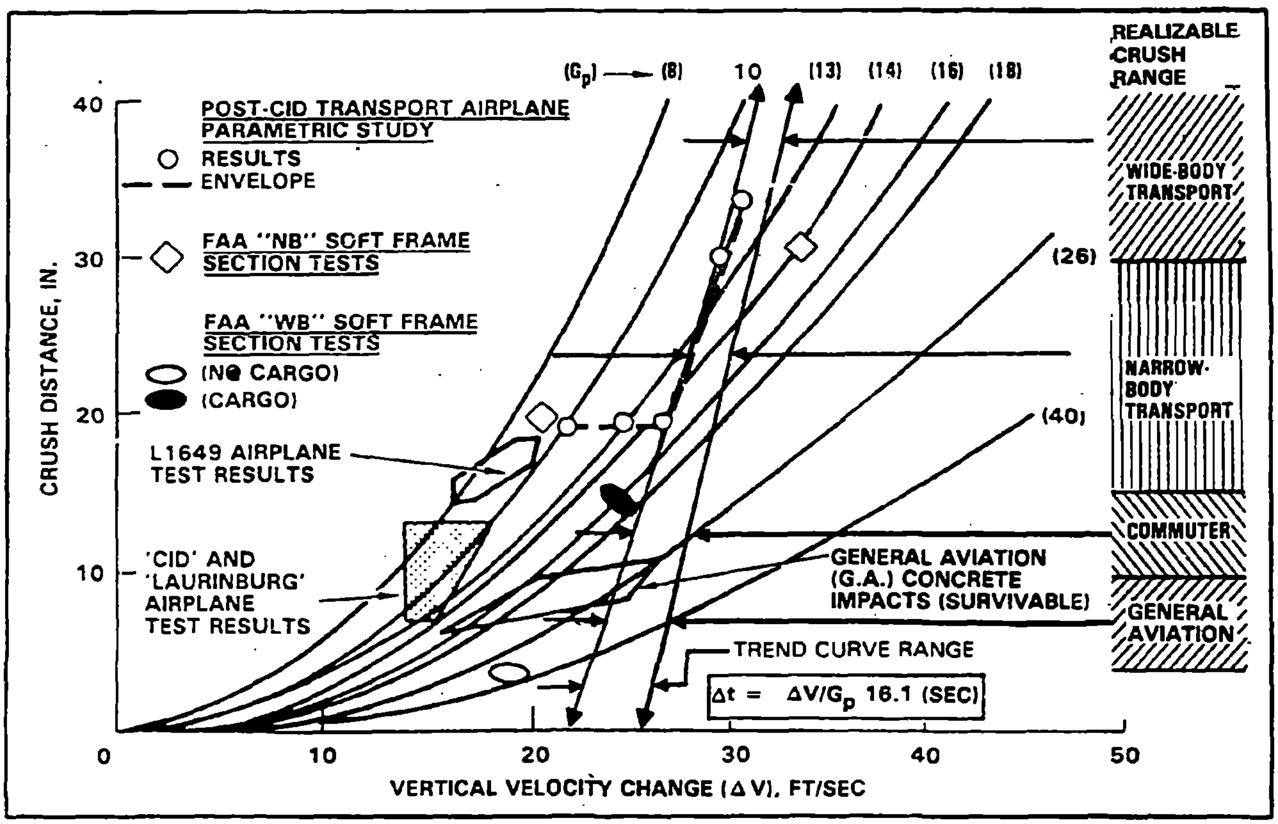

Figure 15. Trend Curve - Vertical Direction Triangular Pulse

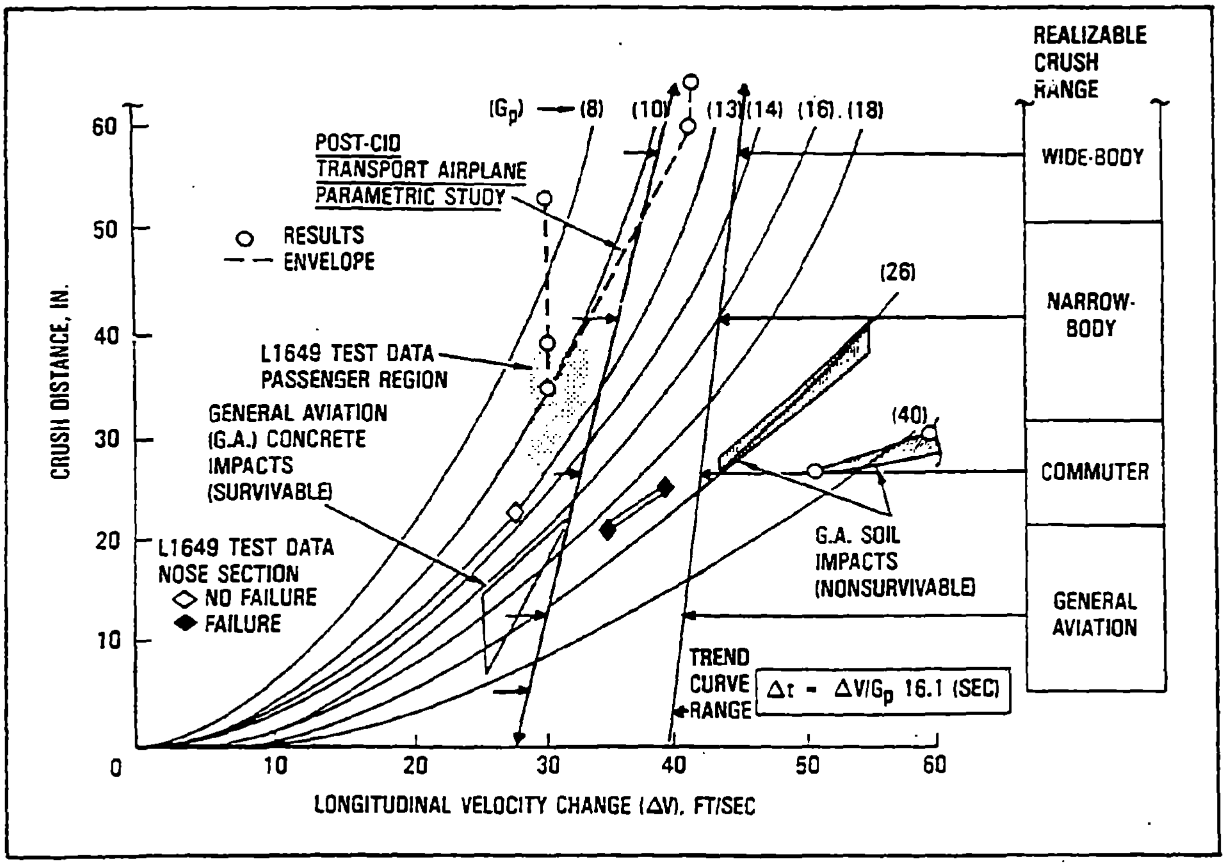

Figure 16. Trend Curve - Longitudinal Direction Triangular Pulse

trend curves assume that the survivable envelope ranges from the fringes of known survivable conditions to FAR 23 nonsurvivable crash test results.

From figure 15 and table 9 it can be observed that an estimate of the average applicable cabin floor dynamic pulses in the vertical direction, based on a mid-range crush capability, are:

33.0 g peak acceleration 26.0 ft/sec velocity change	}	general aviation airplanes
23.0 g peak acceleration 27.0 ft/sec velocity change	}	commuter airplanes
14.0 g peak acceleration 28.0 ft/sec velocity change	}	narrow-body transport airplanes
11.0 g peak acceleration 31.0 ft/sec velocity change	}	wide-body transport airplanes

TABLE 9. RANGE OF FLOOR DYNAMIC PULSES AS A FUNCTION OF AIRPLANE SIZE

AIRPLANE CATEGORY (1)	VERTICAL DIRECTION PULSE			LONGITUDINAL DIRECTION PULSE		
	G_{PEAK}	ΔV FT/SEC	Δt SECONDS	G_{PEAK}	ΔV FT/SEC	Δt SECONDS
GENERAL AVIATION						
LOW	26	24	0.057	26	30	0.072
MIDPOINT	33	26	0.050	33	35	0.066
HIGH	40	28	0.043	10	40	0.062
COMMUTER						
LOW	20	25	0.078	15	33	0.137
MIDPOINT	23	27	0.073	19	37	0.121
HIGH	26	29	0.070	23	41	0.111
NARROW-BODY						
LOW	13	26	0.125	12	36	0.186
MIDPOINT	14	28	0.124	14	39	0.173
HIGH	15	30	0.123	16	42	0.163
WIDE-BODY						
LOW	10	29	0.180	10	38	0.230
MIDPOINT	11	31	0.175	12	41	0.212
HIGH	12	33	0.171	14	44	0.195

(1) PULSES REPRESENTATIVE OF MID-CRUSH REGION FOR RESPECTIVE AIRPLANE CATEGORIES

From figure 16 and table 9 it can be observed that an estimate of the applicable average cabin floor dynamic pulses in the longitudinal direction for all categories aviation airplanes, based on a mid-range crush are:

33.0 g peak acceleration 35.0 ft/sec velocity change	general aviation airplanes
19.0 g peak acceleration 37.0 ft/sec velocity change	commuter airplanes
14.0 g peak acceleration 39.0 ft/sec velocity change	narrow-body transport airplanes
12.0 g peak acceleration 11.0 ft/sec velocity change	wide-body transport airplanes

The size effect data was presented in terms of a range primarily because it is recognized that not every airplane in a particular category has the same available crush depth. For example, from figure 15 if a commuter category airplane has an effective 10 inches of below-floor structural crush the peak acceleration could approach 33g. By the same token, a wide-body transport airplane with over 40 inches of effective vertical crush might not exceed 10g peak acceleration. The size effect study emphasizes that the results are more configuration sensitive and not directly related to mass. Large airplanes with the limited effective crush regions could behave more like smaller airplanes with regard to cabin floor pulses. The parametric study results (reference 18) indicate that the combination of airplane lower fuselage hard (bulkhead) and soft (frame) structure, along with the airplane's impact conditions (sink speed, attitude, terrain, etc.) influence the cabin floor responses. The acceleration-crush-velocity relationship described in this paper for evaluating size effect trends serves to illustrate one methodology that might be used to derive cabin floor crash pulses.

4. CONCLUSIONS

1. Trend Curves have been developed which depict the relationship between fuselage crush distance, velocity change and acceleration levels for different sized airplanes.

2. The trend curves provide an estimate of the range of cabin floor pulse magnitude for general aviation, commuter, narrow-body and wide-body transport airplanes.

3. The size trend curves indicate that the results are configuration sensitive.

4. Measured responses obtained from frame section tests are related to the mass loading density.

5. Additional empirical data and/or modeling results, particularly for cummuter airplanes and high-wing upper mass configurations would be useful in extending the applicability of the proposed trend curves.

5. REFERENCES

1. Amendment Number 23-36, Small Airplane Airworthiness Review Program, Amendment No. 1; Final Rule, Federal Register, Volume 53, No. 157, August 15, 1988.

2. Amendment Numbers 27-5 and 29-29, Occupant Restraint in Normal and Transport Category Rotorcraft, Federal Register, Volume 54, No. 217, November 13, 1989.

3. Notice Number 88-8, Retrofit of Improved Seats in Air Carrier Transport Category Airplanes, Federal Register, Volume 53, No. 95, May 17, 1988.

4. Amendment Number 25-64, Improved Seat Safety Standards, Final Rule, Federal Register, Volume 53, No. 95, May 17, 1988.

5. Federal Aviation Regulations, Part 23, Airworthiness Standards: Normal, Utility, Acrobatic, and Commuter Category Airplanes.

6. Federal Aviation Regulations, Part 25, Airworthiness Standards: Transport Category Airplanes.

7. Federal Aviation Regulations, Part 27, Airworthiness Standards: Normal Category Rotorcraft.

8. Federal Aviation Regulations, Part 29, Airworthiness Standards: Transport Category Rotorcraft.

9. Wittlin, G., Lackey, D., "Analytical Modeling of Transport Aircraft Crash Scenarios to Obtain Floor Pulses," DOT/FAA/CT-83/23, NASA CR 166089, April 1983.

10. Pugliese, S. M., "B707 Fuselage Drop Test Report," Calspan Report No. 7252-1, March 1984.

11. Hayduk, R., Williams, S., "Vertical Drop Test of Transport Fuselage Section Located Forward of the Wing," NASA Tech Memo 85679, August 1983.

12. Johnson, D., Wilson, A., "Vertical Drop Test of a Transport Airframe Section," DOT/FAA/CT-TN 86/34, October 1986.

13. "DC-10 Fuselage Drop Test," Report No. 7251-2, Arvin Calspan report prepared for the FAA Technical Center, Atlantic City, N.J., September 1984.

14. "DC-10 Fuselage Drop Test," FAA Preliminary Data, 1987.

15. Johnson, D., Garodz, L., "Crashworthiness Experiment Summary Full-Scale Transport Controlled Impact Demonstration Program," DOT/FAA/CT-85/20, June 1986.

16. Wittlin, G., LaBarge, W. L., KRASH Dynamics Analysis Modeling - Transport Airplane Controlled Impact Demonstration Test," DOT/FAA/CT-85/9, May 1985 (Revised March 1986).

17. Wittlin, G., "KRASH Analysis Correlation - Transport Airplane Controlled Impact Demonstration Test," DOT/FAA/CT-86/13, December 1986.

18. Wittlin, G., "KRASH Parametric Sensitivity Study - Transport Category Airplanes," DOT/FAA/CT - 87/13, December 1987.

19. Reed, W. H., et al, "Full-Scale Dynamic Crash Test of a Lockheed Constellation Model 1649 Aircraft," FAA Technical Report ADS-38, October 1967.

20. Wittlin, G., Gamon, M. A., "Full-Scale Crash Test Experimental Validation of Methods of Analysis for General Aviation Airplane Structural Crashworthiness," FAA-RD-77-188, February 1978.

21. Vaughan, Jr., V. L., and Hayduk, R. J., "Crash Tests of Four Identical High-Wing Single-Engine Airplanes," NASA Technical Paper 1699, August 1980.

22. Castle, C. B., and Alfaro-Bou, E., "Crash Tests of Three Identical Low-Wing Single-Engine Airplanes," NASA Technical Paper 2190, September 1983.

APPENDIX A

MASS AND SIZE SCALING TRENDS

The following is excerpted from reference A-1. Table A-1 and figure A-1 show the range of weight class and classifications of transport aircraft. Mass, (size) scaling trends are obtained via analysis and are based on the impact conditions and premises noted below. The acceleration versus size effect is shown in figure A-2.

IMPACT CONDITION AND PREMISES

- Six-degree slope
- Forward velocity 172 feet/second
- Rigid ground
- Ground coefficient of friction = 0.70
- The underside crushing spring length is related to the below passenger floor distance
- The fuselage underside crushing force is related to the aircraft fuselage weight
- The fuselage beam properties are obtained from aircraft section properties. Where unavailable they are related to the fuselage cross-section properties as follows:

$$\text{Area} = K_1 \pi r^2 \left[1 - (1 - \frac{t}{r})^2\right]$$

$$\text{Inertia} = K_2 \frac{\pi}{4} r^4 \left[1 - (1 - \frac{t}{r})^4\right]$$

where:

r	=	radius of shell section
t	=	thickness of shell section
K_1, K_2	=	factors determined from available data

The term (t/r) can be thought of as an effective skin thickness ratio and is obtained from available information. It is different for the axial and bending terms. K_1 and K_2 can be developed from known data for different aircraft configurations.

- The fuselage weight properties are obtained from aircraft section-properties. The fuselage stations are located in proportion to the total length. Where unavailable, mass inertia properties are allocated in proportion to aircraft weight distribution.
- Two floor designs are used. One representative of a wide-body aircraft and another representative of a narrowbody aircraft.
- The same general two-passenger seat arrangement is used for all analysis and it is assumed that each seat is fully loaded with 176 pound occupants.

The trend curve noted in figure A-2 is based on the airplane representation modeled in table A-2.

TABLE A-1. AIRPLANE SIZE AND WEIGHT CHARACTERISTICS

Class or Category	Aircraft	Weight x 10^3, Lb. Empty Operating	Zero Fuel	Max. Ldg	Max. T.O.	No. Passengers	Approximate Size, Ft. Fuselage Dia.	Overall Length	Wing Span	Cabin Height	Below PAX Floor	Engine Configuration
B	CV440, 600	31	–	44	57	-56	10	75 – 79	91 – 105	–	3	2
	Viscount-800	41	54	58	73	-67	11	85	94	–	3	4W
	BAC 111	46	71	69	105	-80	11	93	88	–	3	2F
C	L-1649	85	116	123	156	-92	12	116	150	7	4	4W
	B737	65	95	105	126	-115	12	100	93	7	5	2W
	DC-9	50	87	82	147	-90	12	119	93	7	4	2F
	B-727	88	140	142	191	-89	14	133	108	7	5	3F
D	B-720	110	156	175	235	-116	14	137	131	7	7	4W
	B-707	125	230	190	366	-219	14	152	146	7	7	4W
	DC-8	124	180	207	350	-179	14	151	143	7	7	4W
	B757	131	184	198	220	-220	14	155	124	7	7	2W
	B767**	180	248	270	300	-255	16	159	156	8	8	2W
	A300**	195	275	293	363	-345	18	176	147	8	9	2W
E	L-1011**	240	320	358	500	256 – 400*	20	180	155	8	9	2W, 1F
	DC-10**	238	368	363	565	270 – 390*	20	180	155	8	9	2W, 1F
	B-747**	360	525	465	785	385 – 500*	22	231	196	8	10	4W

W = Wing
*All Tourist Configuration

F = Fuselage
**Wide-body aircraft

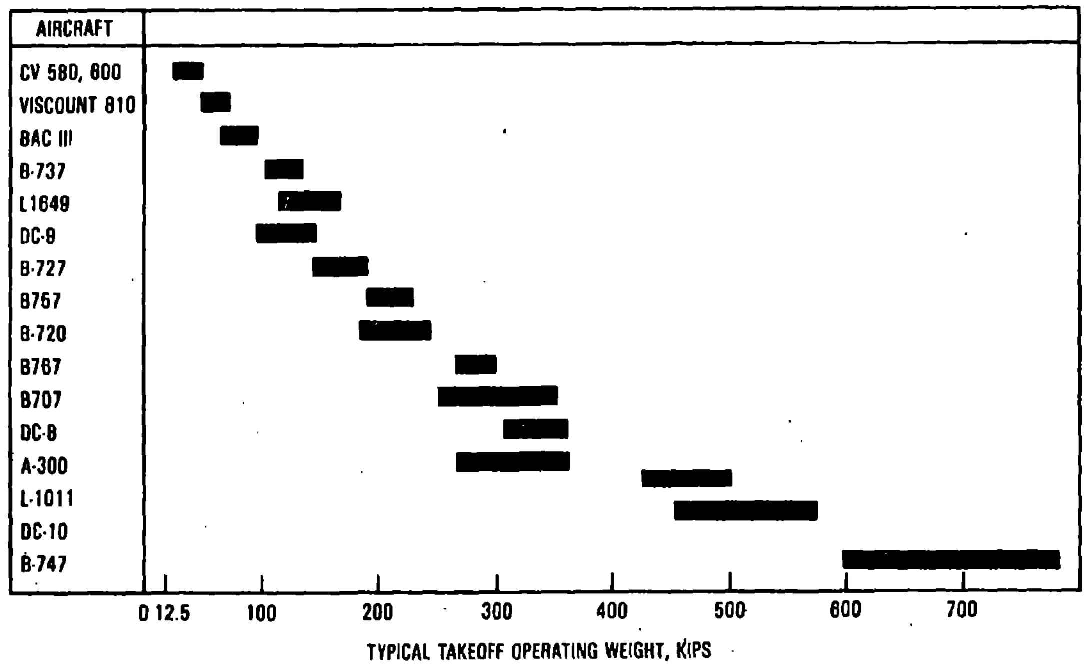

Figure A-1. Transport Airplane versus Takeoff G.W.

TABLE A-2. AIRPLANE REPRESENTATIONS MODELED

REPRESENTATION	WEIGHT LB x 10^3	FUSELAGE DIA., IN.	OVERALL FUSELAGE LENGTH, IN.	MAXIMUM UNDERFLOOR DISTANCE, IN.
B TYPE	80	130	1020	40
C TYPE	159	140	1367	50
*D TYPE	175–220	170	1566	78
*D TYPE	245–320	170	1746	78
E TYPE	328–432	220	2127	100

*ANALYSIS TO BE PERFORMED IN CONJUNCTION WITH B720 CRASH TEST PROGRAM

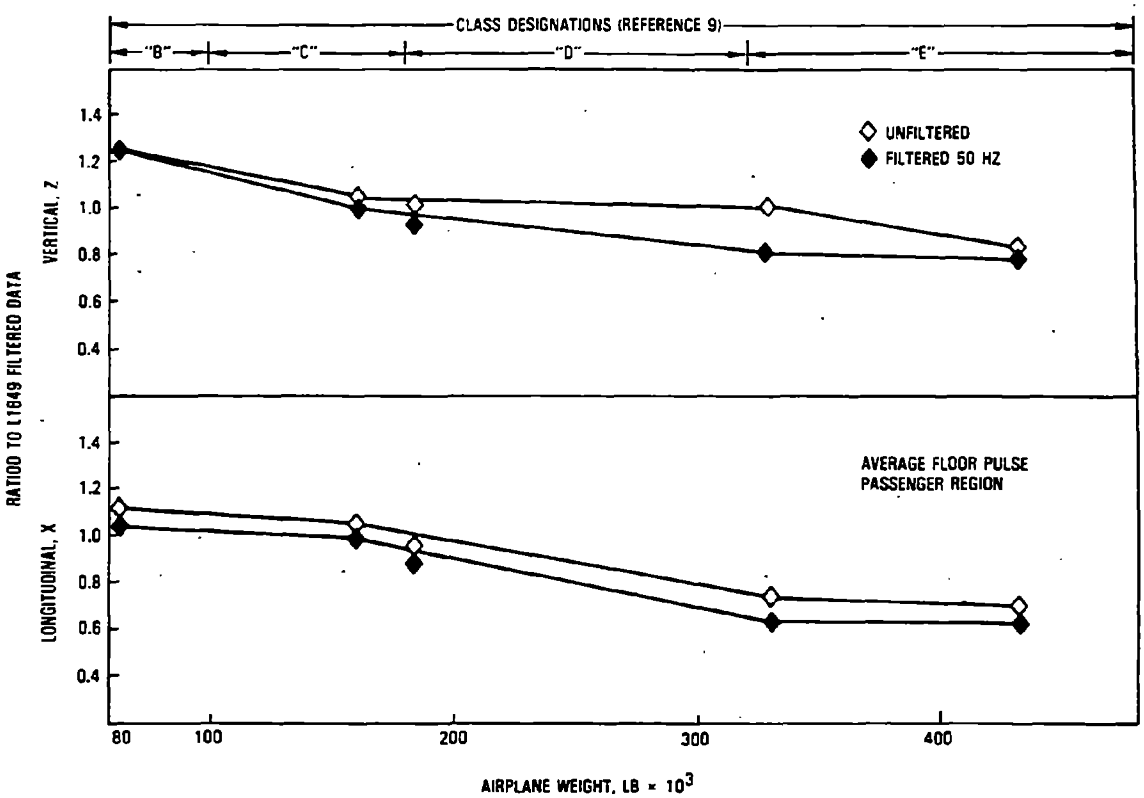

Figure A-2. Acceleration vs Weight (Size) Trend

REFERENCES

A-1 "Analytical Modeling of Transport Aircraft Crash Scenario to Obtain Floor Pulses," DOT/FAA/CT-83/23, NASA CR/66089, April 1983

APPENDIX B

LIGHT FIXED-WING AIRPLANE (FAR 23) TEST RESULTS

Four light high-wing single-engine FAR 23 airplanes (GTOW-2700 pound) were crash tested at the NASA Langley Impact Dynamics Facility in the mid-1970's as part of a FAA sponsored research effort. The FAA program, including analyses and test results, is described in reference B-1. The tests are summarized in reference B-2. The two tests in the sequence that are of particular interest have impact parameters as shown in table B-1.

TABLE B-1. TEST IMPACT PARAMETERS

Test Number	1	4
Terrain	Concrete	Soil
Impact Velocities (feet/ second		
Flight path	81.4	82
Longitudinal	69.5	71
Vertical	42	46.8
Angles (degrees)		
Flight path	-30.72	-32
Impact	-30.17	-34.8
Attack	0.57	-2.8
Roll	+4.13	<1.0
Yaw	-3.27	<1.0

Figures B-1 through B-4, obtained from reference B-2, help describe the results of the test Number 1 impact onto a concrete surface. The impact sequence, shown in figure B-1 shows how the airplane, after contacting the ground, crushes in the forward end, rotates slightly and continues to slide out. The locations of the accelerometers on the airplane, for this and other three tests in the sequence, are shown in figure B-3. The accelerometer time-histories recorded for this test are provided in figure B-4 (two pages). The measured cabin floor and firewall accelerations in the airplane normal direction indicate a primary pulse of:

peak acceleration, g_p = 15g to 25g
velocity change, ΔV = 14 feet/second to 24 feet/second
base time duration, Δt = .06 seconds

A secondary pulse occurs which exhibits a lower magnitude and, correspondingly, lower velocity change. However, the response of seat/occupant systems exposed to the floor pulse can be much different for a short pulse than for a longer pulse. This data is for a severe but survivable crash impact condition.

The test Number 1 results, for the impact onto the concrete surface, indicate the followed approximate representative cabin floor longitudinal pulses:

	①	②	③
g_p	20	30	40*
Δt, second	.07 - .10	.05	.04
ΔV, feet/second	22 - 32	24	26

* firewall floor

The test Number 4 results, for the impact onto soil, are depicted in figures B-5 through B-7. The impact sequence, shown in figure B-5, shows that the airplane initially digs into the soil and then overturns. The initial forces are primarily along the airplane longitudinal axis and cause extreme crushing of the forward region, back to the pilot's floor, as is noted in figure B-6. The recorded acceleration responses (figure B-7) show extremely high longitudinal forces and little in the way of normal accelerations during this initial impact phase, as one would expect from the manner in which the airplane behaves during the sequence. The normal traces measuring airplane normal acceleration indicates a down acceleration as exposed to upward deceleration. This most likely indicates the airplane rotating as opposed to crush forces.

The acceleration longitudinal pulses (figure B-7) for the impact onto soil approximate to the following pulses:

	①	②	③
G_p	40	40	45
Δt, second	.07	.08	.07
Δv, feet/second	45	51	52

This pulse range is shown in figure 14 of the main text. From the plot in figure 14, approximately 20-28 inches of crush is needed to produce the pulses noted above within .15 seconds after initial ground contact. The post-test observations show that the fuselage forward of the firewall has been demolished, the engine torn loose and the firewall has been pushed back compressing the cabin compartment. This particular impact condition is considered non-survivable.

REFERENCES

B-1 "Full-Scale Crash Test Experimental Verification of Methods of Analysis for General Aviation Airplane Structural Crashworthiness," FAA-RD-77-188, February 1978

B-2 "Crash Tests of Four Identical High-Wing Single-Engine Airplanes," NASA Technical Paper 1699, August 1980

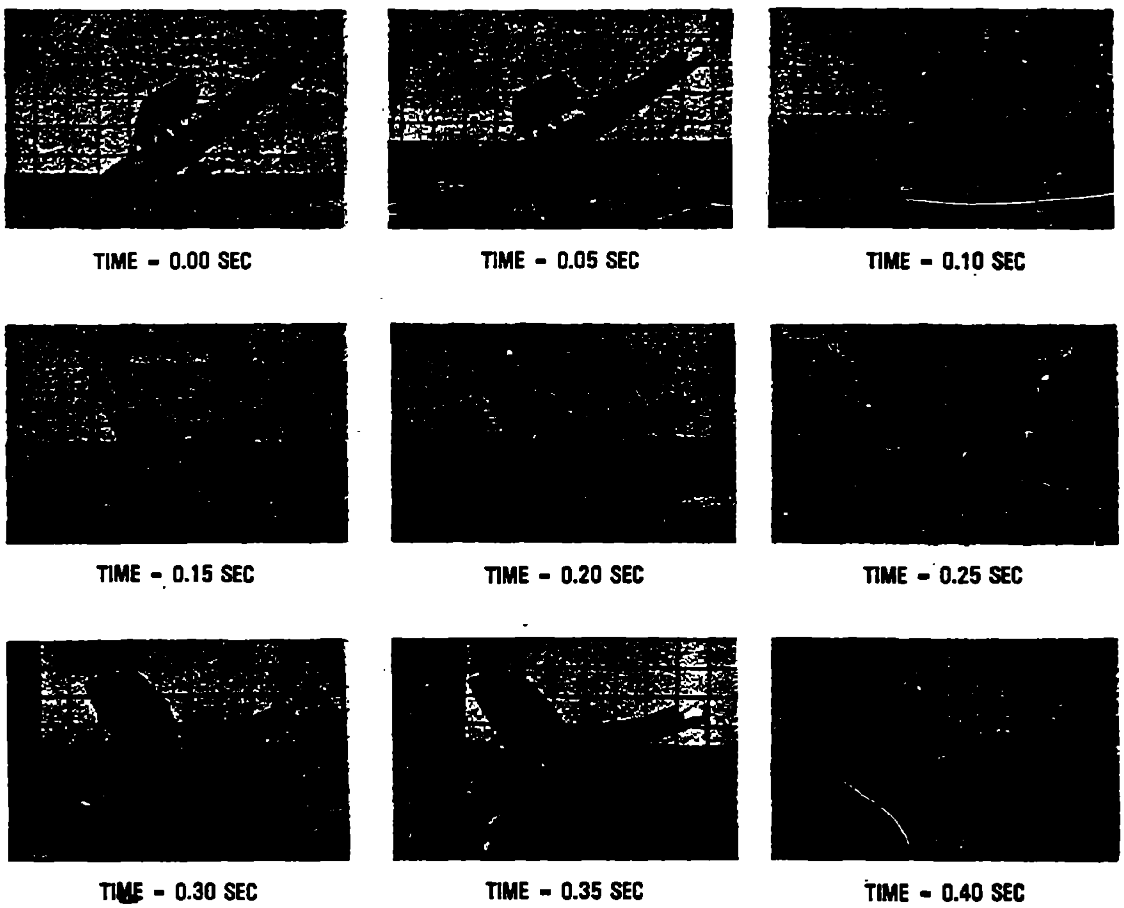

Figure B-1. Crash Sequence Photographs of Nose-Down Test

ORIGINAL PAGE
BLACK AND WHITE PHOTOGRAPH

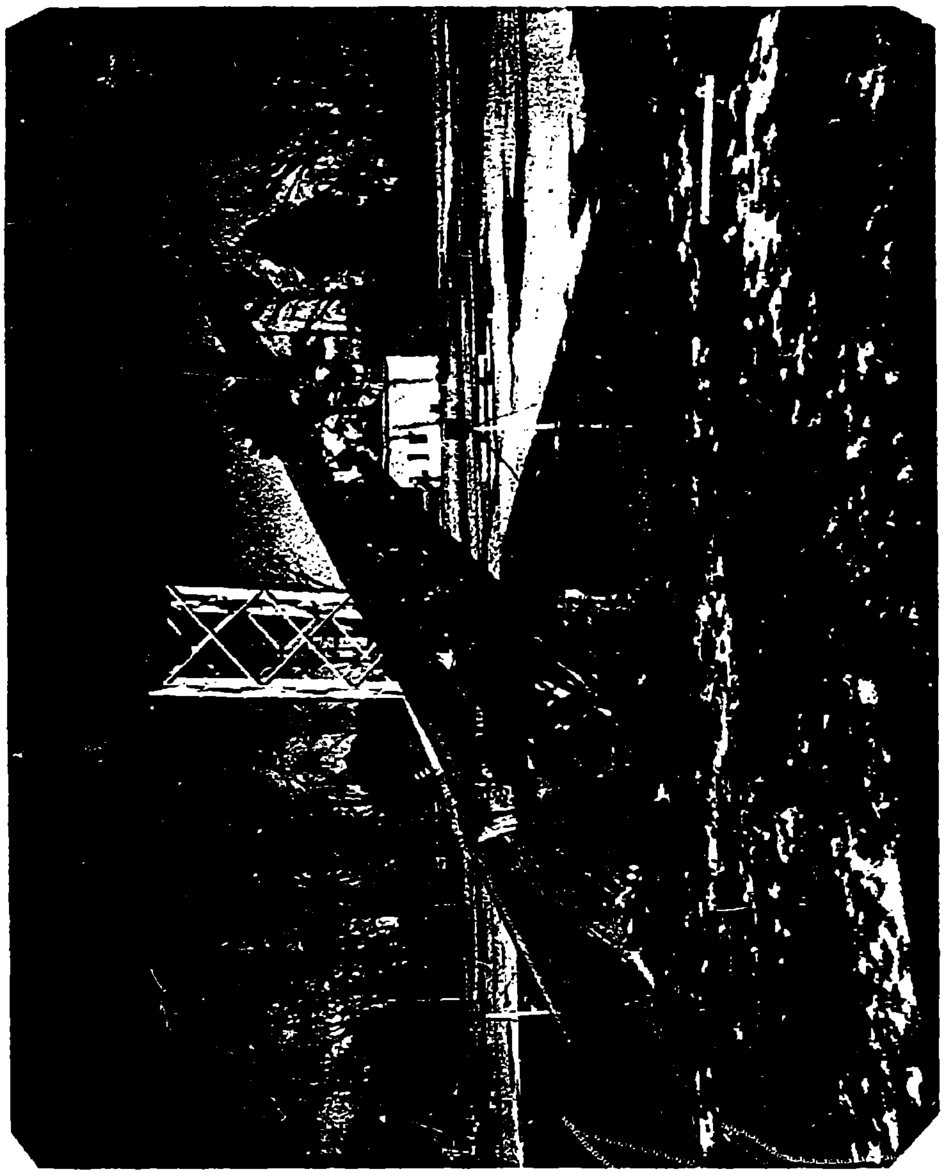

Figure B-2. Postcrash Damage of Nose-Down Test

ORIGINAL PAGE IS
OF POOR QUALITY

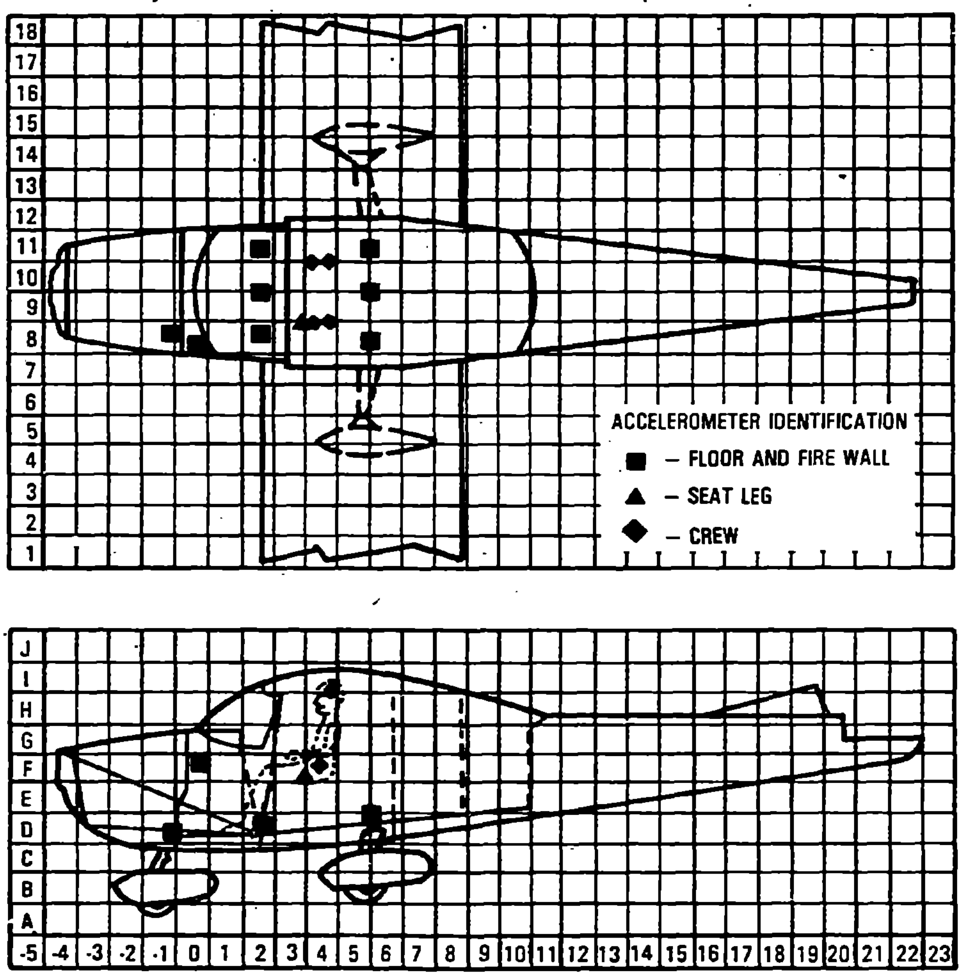

ACCELEROMETERS IN DUMMIES

PILOT, PELVIC, NORMAL*	4F8N	COPILOT, PELVIC, NORMAL	4F11N
PILOT, PELVIC, LONGITUDINAL**	4F8L	COPILOT, PELVIC, LONGITUDINAL	4F11L
PILOT, HEAD, NORMAL	8I8N	COPILOT, HEAD, NORMAL	4I11N
PILOT, HEAD, LONGITUDINAL	4I8L	COPILOT, HEAD, LONGITUDINAL	4I11L

* ALONG SPINE
** PERPENDICULAR TO SPINE

Figure B-3. Diagram of Accelerometer Locations on Airplane Structure and in Dummies

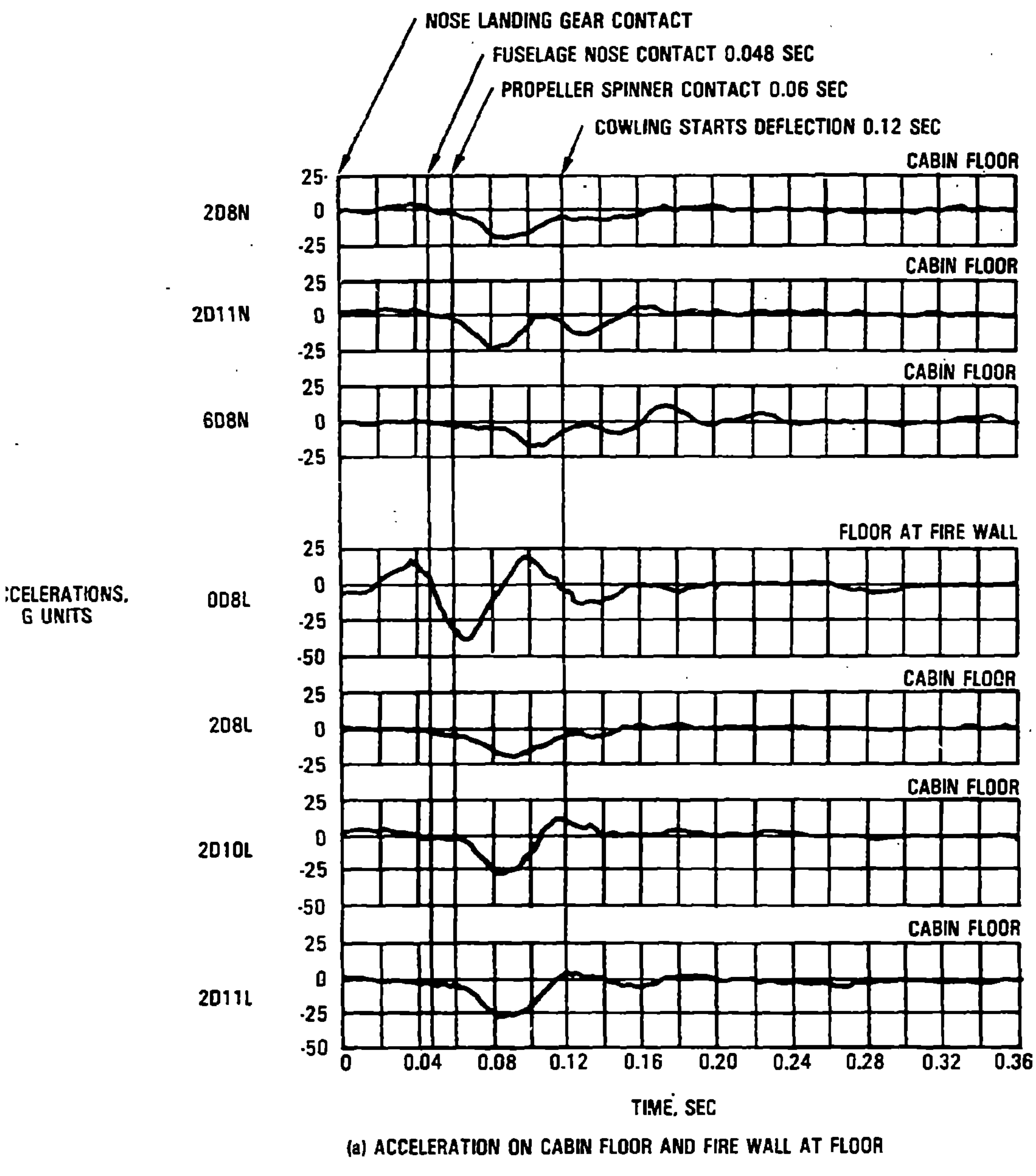

Figure B-4. Acceleration and Load Histories Onboard Nose-Down Test Specimen (1 of 2)

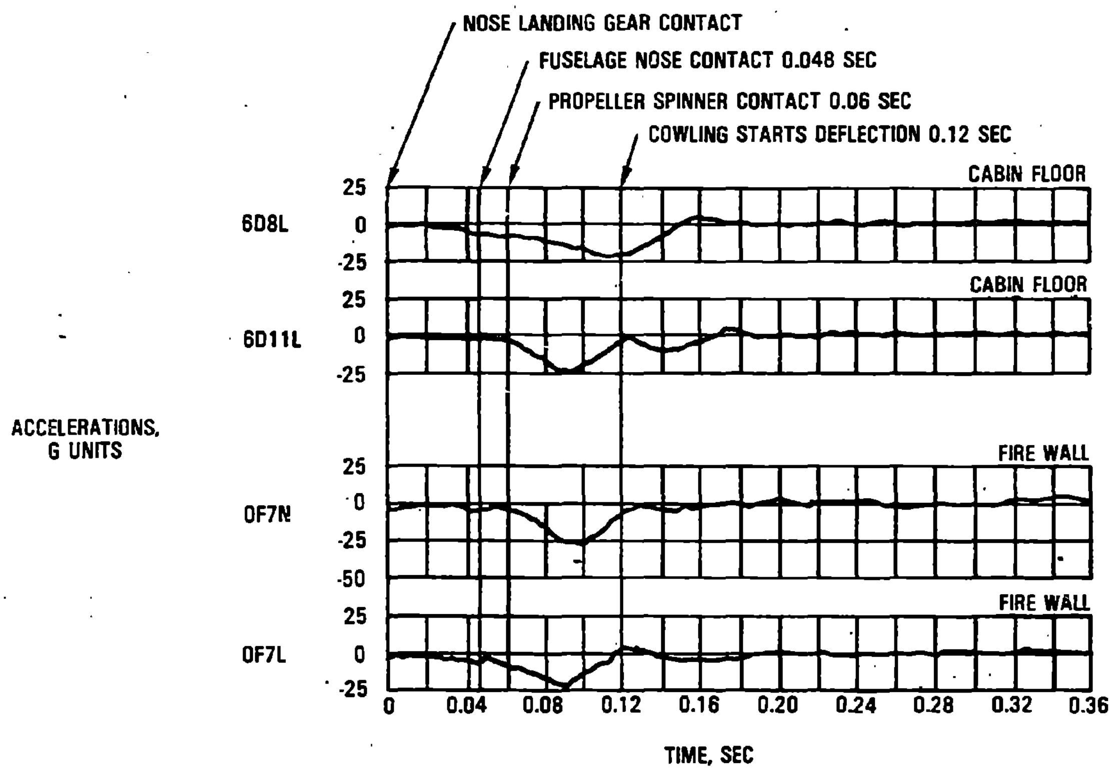

(b) ACCELERATIONS ON CABIN FLOOR AND ON FIRE WALL

Figure B-4. Acceleration and Load Histories Onboard Nose-Down Test Specimen (2 of 2)

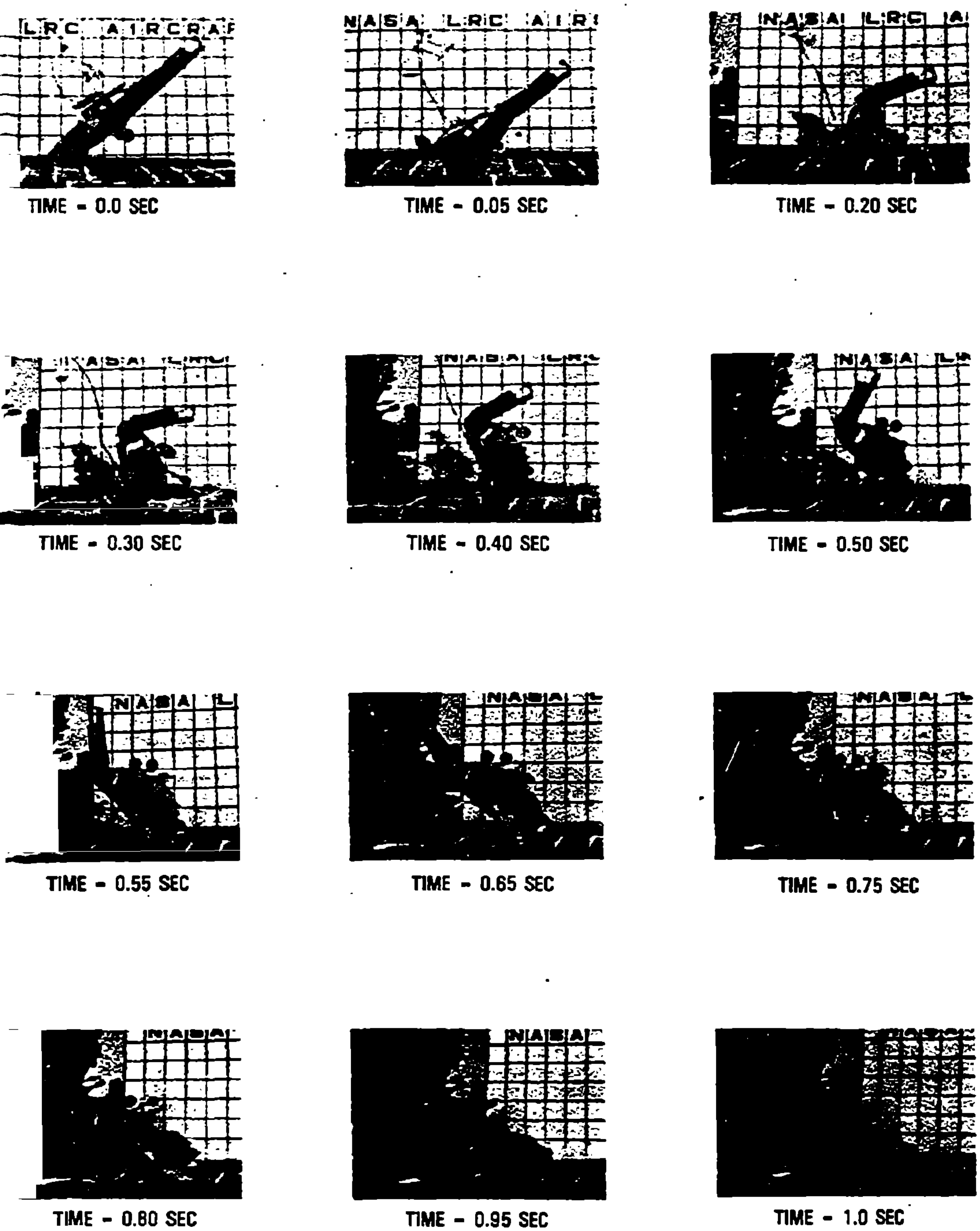

Figure B-5. Crash Sequence Photographs of Nose-Down-on-Soil Test

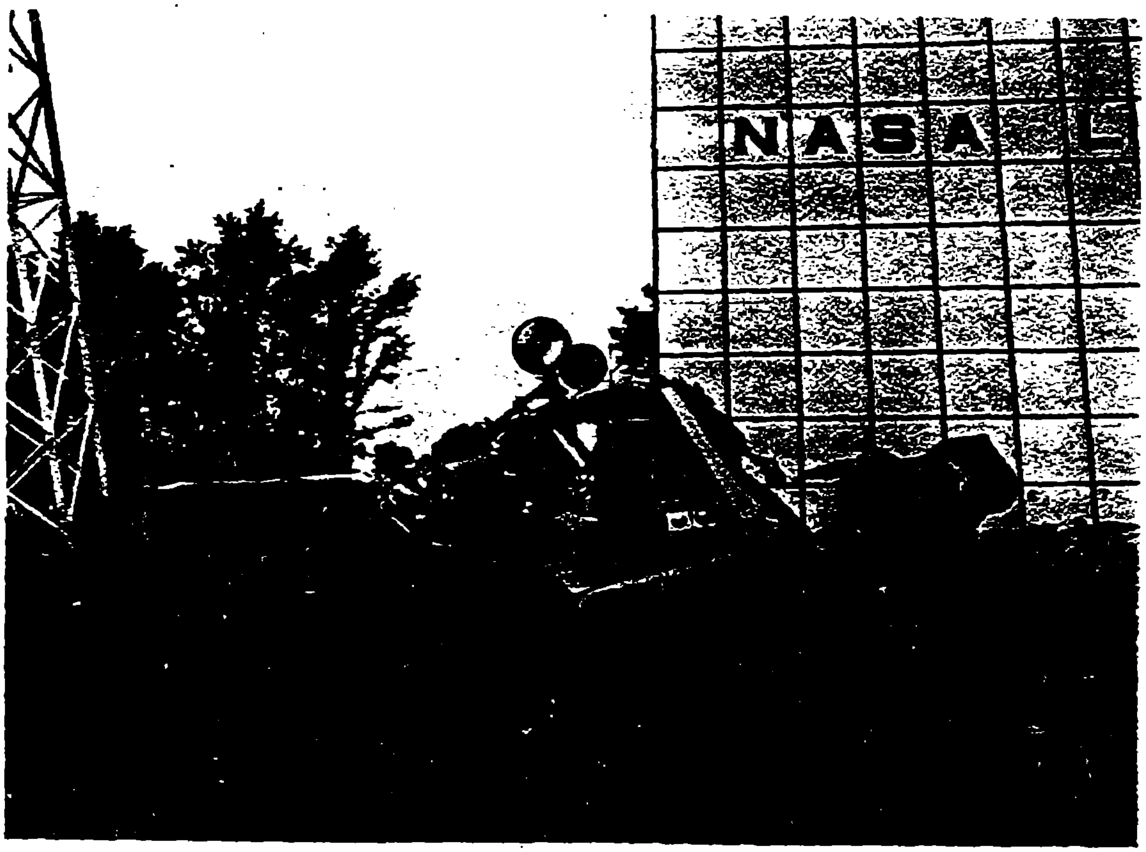

(a) View of port side of airplane.

Figure B-6. Postcrash Damage of Nose-Down-on-Soil Test

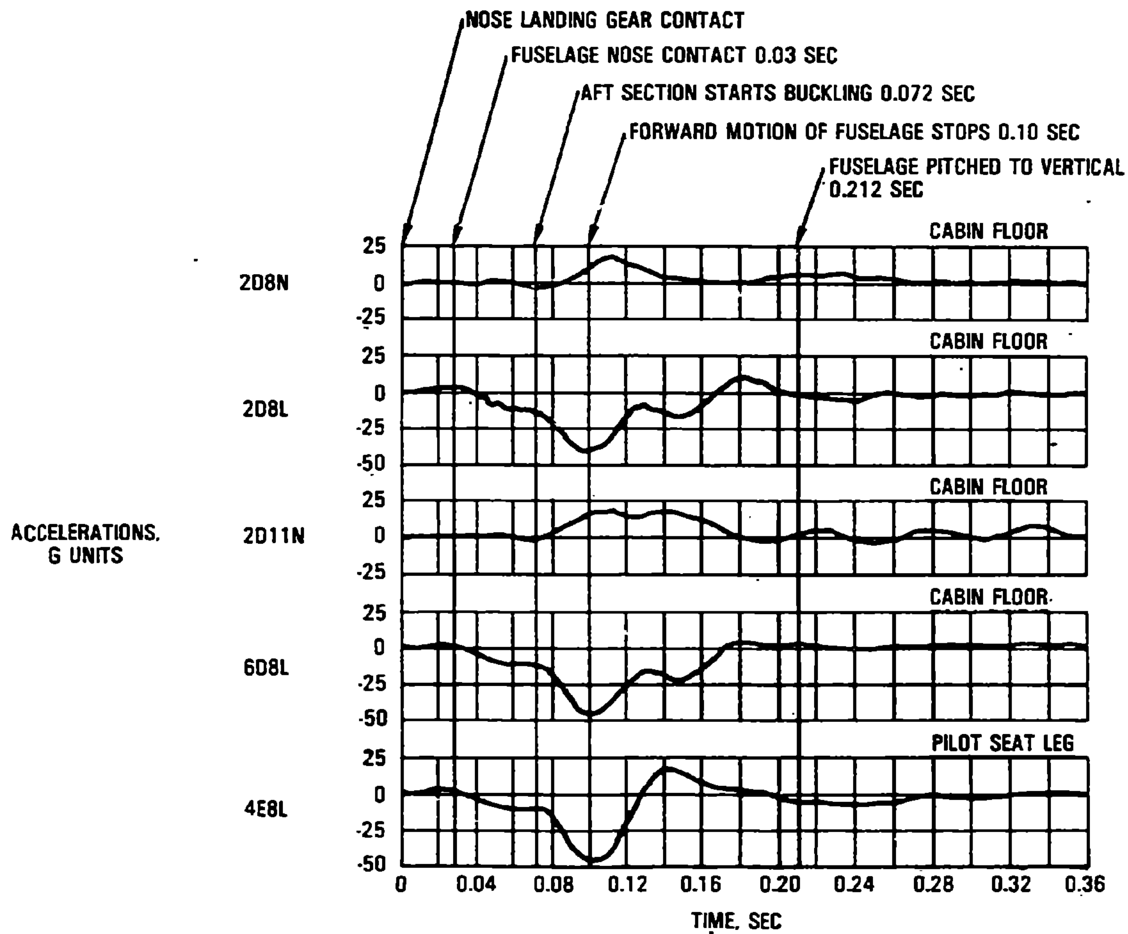

(a) Acceleration on cabin floor and pilot's seat leg.

Figure B-7. Acceleration and Load Histories Onboard Nose-Down-on-Soil Test Specimen

*U.S. GOVERNMENT PRINTING OFFICE: 1990-704-061/20085